Research and implementation of multi-dataset training for image classification with discrepant taxonomies

A master thesis in the field of computer science

by

Björn Buschkämper

1st supervisor: Dr. Petra Bevandic

2nd supervisor: M.Sc. Riza Velioglu

Submitted in the research group "HammerLab"
of the faculty of technology for the degree of
Master of Science
at
Universität Bielefeld

September 6, 2025

Contents

I Introduction

Image classification is one of the earliest and most widely researched tasks in computer vision. It involves assigning a label to an image from a predefined set of categories. Over the years, numerous approaches have been proposed to tackle this problem, ranging from traditional handcrafted feature-based methods to modern deep learning techniques.

A major limitation in image classification is the restricted range of categories that a single model can effectively recognize. This limitation arises because most traditional models are trained on specific datasets with predefined class sets. To address this issue, researchers have explored various strategies to make a single model applicable to a broader range of datasets and categories.

One of the most common approaches is transfer learning. Transfer learning operates under the assumption that models trained on large general-purpose datasets (e.g., ImageNet [5, 33]) have learned fundamental visual features (such as shapes and textures) that are useful for any downstream task. By replacing the final classification layer of these pre-trained models with a task-specific layer, researchers can adapt the model to new categories without training from scratch [31, 44].

However, this approach still results in separate models for each task, which is inefficient in terms of storage and deployment. One way to address this is through shared backbone architectures, where a single model extracts features from input data (the "backbone"), and multiple task-specific "heads" are added on top for different tasks. This approach leverages commonalities between tasks and enables more efficient resource usage [38].

Multi-task learning extends this technique by training a single model on multiple tasks simultaneously. This approach enforces the learning of shared concepts and representations across tasks, potentially leading to improved performance and generalization [43]. However, this approach relies on automatic distillation of shared features, which can be challenging depending on task domain alignment.

We address this issue by first building a map of shared concepts and features across tasks, then using this map to train a single universal model that works for all targeted tasks without task-specific adaptations or layers. This approach enforces predefined shared concepts and features to be learned by the model, rather than relying on automatic distillation.

Our first challenge is finding an accurate mapping of shared concepts and features across tasks. This mapping should be created without manual intervention. Key challenges include:

- Creating a method that distinguishes where shared concepts and features exist across domains and where no relations exist. Depending on the domains, there can be significant variations in inter-task similarity, potentially limiting the number of shared concepts and features.

- Defining a consistent threshold for what constitutes a shared concept or feature. The definition of a "shared concept" varies greatly depending on the task combination: General-purpose datasets like ImageNet and CIFAR-100 might share straightforward concepts like "cat" and "dog" (shared concept "animals"), while specialized datasets may have no overlap and rely on entirely different concepts (such as specific textures or patterns). Our method must identify the best-matching concepts and features across these diverse datasets.

After creating a mapping of shared concepts and features, we use this information to guide the training of our universal model. We build a custom learning function that uses the mapping to create a single, shared output layer for all tasks. This output layer can then be converted to create task-specific predictions based on a static function, eliminating the need for task-specific learning.

We compare the performance of our universal model against baseline models trained on individual domain datasets. In this thesis, we focus on general-purpose datasets such as ImageNet [5, 33], CIFAR-10 and CIFAR-100 [25], and Caltech-101 and Caltech-256 [13, 27].

Additionally, we compare our relationship mapping methods against the existing taxonomy creation method by Bevandic et al. [1, 2] and discuss their respective strengths and weaknesses.

2 Related Work

This chapter provides a comprehensive overview of the existing literature related to multi-dataset training for image classification with discrepant taxonomies. We organize the related work into several key areas that form the foundation of our research: label alignment and taxonomy learning, multi-domain learning approaches, knowledge transfer between datasets, and automated taxonomy construction methods.

2.1 Multi-Dataset Training and Domain Adaptation

Multi-dataset training has emerged as a critical research area in computer vision and machine learning, driven by the need to leverage diverse data sources for improved model generalization [42]. The fundamental challenge lies in reconciling different labeling schemes, annotation quality, and domain-specific biases across datasets.

Traditional domain adaptation approaches focus on adapting models trained on a source domain to perform well on a target domain [11, 39]. However, these methods typically assume correspondence between domains, either through shared label spaces or overlapping features. Multi-dataset training with discrepant taxonomies requires more sophisticated approaches that can handle completely different categorization schemes.

Universal models that can operate across multiple datasets simultaneously have gained significant attention [23, 32]. These approaches typically rely on large-scale pretraining followed by fine-tuning, but they often struggle with datasets that have fundamentally different organizational principles.

2.2 Label Alignment and Taxonomy Learning

The challenge of aligning labels across datasets is fundamental to our work. We base our method for finding shared concepts between datasets on established works in label alignment and taxonomy learning. Creating connections between datasets is important in machine learning: Many datasets are created for specific tasks and may not be directly comparable. Additionally, inconsistencies in labeling and data collection practices can further complicate dataset integration. Meth-

ods for creating dataset connections can help align labels, improve data quality, and facilitate knowledge transfer between models trained on different datasets.

2.2.1 Manual and Semi-Automated Approaches

The most straightforward approach for aligning labels across datasets is manual mapping from one dataset to another. While providing high accuracy when performed by domain experts, this method is time-consuming and error-prone, especially for large datasets. Manual annotation also introduces inconsistencies when multiple annotators are involved or when datasets are updated independently over time [3, 21, 41].

Snow et al. [34] demonstrated that crowdsourcing can be effective for certain annotation tasks, but the quality of manual alignments varies significantly with annotator expertise and task complexity. This variability becomes particularly problematic when dealing with fine-grained taxonomic distinctions or domain-specific terminology.

An improvement over purely manual approaches is a hybrid method that operates automatically but incorporates manual corrections. For example, Firmani et al. [10] propose a weakly supervised approach where domain experts answer targeted questions about datasets to guide automated label alignment. This method balances automation and human expertise, leveraging the strengths of both approaches while minimizing required manual effort.

2.2.2 Large Language Model-Based Approaches

With the rise of large language models (LLMs), new methods have emerged that replace human domain experts with automated systems. These systems leverage the capabilities of LLMs to understand and align labels across datasets without the need for human input, creating a pseudo-hybrid approach where the human role is replaced with sophisticated language understanding [4, 14, 22].

Kargupta et al. [22] introduced TaxoAdapt, which uses large language models to automatically generate taxonomic alignments between datasets. Their approach demonstrates significant improvements over baseline methods but requires careful prompt engineering and may inherit biases present in the language model's training data.

Chen et al. [4] explored the use of prompting strategies for cross-dataset label alignment, showing that well-designed prompts can elicit meaningful semantic relationships from pre-trained language models. However, their work also highlights the challenges of ensuring consistency and accuracy in LLM-generated alignments.

2.2.3 Automated Non-LLM Approaches

For fully automated, non-LLM-based approaches, several different methodologies have been developed:

WordNet-Based Methods: WordNet is a lexical database that groups English words into sets of synonyms called synsets, providing short definitions and usage examples [9, 40]. It can be used to find relationships between words and concepts, making it a valuable resource for aligning labels across datasets. WordNet has been extensively used in various natural language processing and computer vision tasks for establishing semantic relationships, the most popular example being the ImageNet database [5].

However, as we will later demonstrate in Section 4.2.1, this method is error-prone and not suitable for all datasets. WordNet's coverage is limited to English and may not capture domain-specific terminology or modern usage patterns. Furthermore, the hierarchical structure of WordNet may not align with the organizational principles of specific datasets.

Cross-Domain Classification Methods: These approaches use models trained on a specific dataset to create cross-domain predictions and infer label relationships [1, 2, 37]. For example, if dataset *A* has a class *A:vehicle* while dataset *B* has a class *B:car*, by predicting an image from class *B:car* using a model trained on dataset *A* as *A:vehicle*, we can collect cross-domain co-occurrences and build a mapping between the two datasets.

This approach has the advantage of being grounded in actual model behavior and data distributions, making it more robust to semantic inconsistencies that might not be captured by purely linguistic approaches. However, it requires sufficient model performance across domains and may be sensitive to domain shift effects.

2.3 Knowledge Transfer and Representation Learning

Knowledge transfer between datasets with different taxonomies is closely related to the broader field of transfer learning and representation learning. The key insight is that while surface-level labels may differ, underlying visual features and semantic concepts often exhibit significant overlap across datasets.

2.3.1 Feature-Based Transfer Methods

Donahue et al. [7] demonstrated that features learned on large-scale datasets like ImageNet can transfer effectively to other visual recognition tasks. This work established the foundation for using pre-trained features as a bridge between different datasets and taxonomies.

More recent work has explored how to adapt these pre-trained representations to better capture the specific taxonomic structures of target datasets [15, 24]. These approaches typically in-

volve fine-tuning strategies that preserve useful general features while adapting to dataset-specific requirements.

2.4 Our Approach in Context

We will base our taxonomy construction algorithm on the works of Bevandic et al. [1, 2], who proposed cross-domain classification methods for automatic label alignment. Their approach uses trained models to establish correspondences between datasets by analyzing prediction patterns across domains.

Our method will be adapted to shift the focus from aligning labels in a universal cross-domain taxonomy towards building relationships between classes in different datasets. Importantly, relationships will not, as in the original work, define a strict hierarchical structure, but rather point out shared attributes and semantic similarities between classes. This adaptation is motivated by the observation that many real-world datasets organize concepts in ways that are not naturally hierarchical but rather reflect different perspectives on the same underlying visual domain.

By building on these established foundations while addressing their limitations, our approach aims to provide a more flexible and robust solution for multi-dataset training with discrepant taxonomies. The following chapters will detail our specific methodology and demonstrate its effectiveness across various datasets and domains.

3 Methodology

Our main goal is to create a universal taxonomy that connects multiple image classification datasets. This taxonomy maps every dataset class to a universal class, enabling us to analyze relationships and shared concepts between datasets.

Ultimately, our taxonomy will allow us to train models that can classify images from multiple datasets simultaneously, building a robust and flexible system that can adapt quickly to new domains.

3.1 Formal Definitions

To formalize our algorithm for building a universal taxonomy, we first define key terms:

- **Dataset** D: A collection of images and labels written as $D = \{(x_1, c_1), (x_2, c_2), \dots, (x_n, c_n)\}$, where x_i is an image and c_i is its label. For multiple datasets, we use indexing: $D_i = \{(x_1^i, c_1^i), (x_2^i, c_2^i), \dots, (x_n^i, c_n^i)\}$, where D_i is dataset D with index i. We denote the set of all classes in a dataset as $C_i = \{c_1^i, c_2^i, \dots, c_k^i\}$.
- **Model** m: A neural network trained on a dataset D_I which maps an image $x \in X$ to a class $c_i^I \in C_I$, denoted as $m_I : X \mapsto C_I$.
- **Domain**: Since both models and classes are dataset-specific, we define **domain** as dataset D_i and its classes C_i.
- **Universal Classes**: Our universal taxonomy will contain a set of classes that are not specific to any dataset. We denote these classes as $C_U = \{c_1^U, c_2^U, \dots, c_k^U\}$. A universal class is a concept represented by a set of domain classes that share similar characteristics. We therefore define a function classes : $C_U \mapsto \mathcal{P}(C)$, where $\mathcal{P}(C)$ is the power set of C, to represent the set of domain classes that belong to a universal class.
- **Graph**: We represent our taxonomy as a directed graph $G = (V, E)$, where V is a set of vertices and E is a set of edges. Each vertex v_i represents a single class or universal class, which we define with class : $V \mapsto C$. Every edge e_{ij} between two vertices v_i and v_j indicates a relationship class$(v_i) \rightarrow$ class(v_j).

- **Probability**: Every edge e_{ij} has a probability associated with it, which indicates the likelihood of classifying an image from class class(v_i) as class class(v_j). We denote this as a function probability : $E \mapsto [0, 1]$.

3.2 Cross-Domain Graph Generation

Before building our universal taxonomy, we need to construct our initial graph that captures the relationships between classes across different domains:

1. **Foreign predictions**: For each dataset with its corresponding model, we run the model on all images from all other datasets. This gives us a set of predictions $P_{ab} = \{(x_i^a, c_j^b)\}$, where x_i^a is an image from dataset D_a and c_j^b is the class predicted by model m_b for that image.

2. **Prediction probabilities**: We count the number of times each class c_i^a was predicted as a foreign-domain class c_j^b. We denote this count in a matrix $M_{ab} \in \mathbb{N}^{+|C_a|\times|C_b|}$, where $M_{ab}(i, j)$ is the number of times class c_i^a was predicted as class c_j^b. We then divide each entry in the matrix by its row sum to get the probability of classifying an image from class c_i^a as class c_j^b:

$$P_{ab}(i, j) = \frac{M_{ab}(i, j)}{\sum_{k=1}^{|C_a|} M_{ab}(i, k)}$$

   This gives us a matrix $P_{ab} \in [0, 1]^{|C_a|\times|C_b|}$, where $P_{ab}(i, j)$ is the probability of classifying an image from class c_i^a as class c_j^b.

3. **Graph construction**: We now create a directed graph that represents the relationships between classes and datasets by iterating over every dataset D_a with every dataset D_b where $a \neq b$ for cross-predictions:

   a) We want to evaluate different methods for selecting the most relevant relationships, so we formalise a function select_relationships(P_{ab}) : $[0, 1]^{|C_a|\times|C_b|} \mapsto \mathcal{P}(\mathbb{N}^2)$ that selects a set of relationships from the probability matrix P_{ab}.

   b) For every $(i, j) \in$ select_relationships(P_{ab}):

      i. We create the vertices v_k and v_l for classes c_i^a and c_j^b respectively if they do not already exist and add them to the graph (otherwise we find the existing vertices for these classes as v_k and v_l).

      ii. We create an edge e_{kl} between the vertices v_k and v_l and add it to the graph.

      iii. We define probability(e_{kl}) = $P_{ab}(i, j)$.

3.2.1 Selecting Relationships

To now filter relationships from the probability matrix, we define a range of different methods and later evaluate their performance.

Our main challenges are:

- **Unknown number of shared concepts**: We don't know how many concepts two classes from different domains share, so we do not know how high the probability of a relationship should be.
- **Noisy predictions**: A low model accuracy can severely impact the relationship predictions, since - depending on the number of foreign classes that share concepts with the class - the target probabilities can be very low, making even a small number of wrong predictions a huge obstacle.
- **Unbalanced datasets**: Some datasets might have more images for a class than others, which can lead to skewed probabilities. This can be mitigated by preprocessing the datasets to balance the number of images per class, but our goal is to create a methodology that can be applied to any dataset without specific requirements on the datasets.

Naive Thresholding

The most straightforward method is to apply a fixed threshold to the probabilities:

$$\text{select\_relationships}(P_{ab}) = \{(i, j) \mid P_{ab}(i, j) \geq t\}$$

where t is a threshold value between 0 and 1.

Most Common Foreign Predictions

As in the paper that provided the ground work for our methodology [2], we can also select the single most common foreign prediction for each class:

$$\text{select\_relationships}(P_{ab}) = \{(i, j) \mid j = \text{argmax}_{j'} P_{ab}(i, j')\}$$

Density Thresholding

Another approach is to use the least amount of relationships whose summed probabilities cover a certain percentage of the total probability mass. This can be done by sorting the probabilities in descending order and then selecting the smallest set of relationships that covers at least p percent of the total probability mass:

1. We define $R = \emptyset$ as the set of relationships to select.
2. For every $i \in \{1, \dots, |C_a|\}$:
   a) Let X_i be the list of all probabilities in row i of P_{ab} sorted in descending order.
   b) We find the smallest k such that $\sum_{j=1}^{k} X_i(j) \geq p$.
   c) We add the first k relationships of the sorted list X_i to R.
3. We return R for the function select_relationships(P_{ab}).

Relationship Hypothesis

Let us naively assume that every relationship between two classes is based on a single shared concept. In this case, the probability of every outgoing edge from a class c_i^a should be roughly equal.

We can therefore hypothesise the probability distribution based on the number of relationships and compare this hypothesis against the actual probabilities in the matrix P_{ab}:

1. We define $R = \emptyset$ as the set of relationships to select.
2. For every $i \in \{1, \dots, |C_a|\}$:
   a) Let X_i be the list of all probabilities in row i of P_{ab} sorted in descending order.
   b) We find the $k \in \{1, \dots, n\}$ such that we minimise:

$$\sum_{j=1}^{k} \left| X_i(j) - \frac{1}{k} \right| + \sum_{j=k+1}^{|C_b|} X_i(j)$$

   c) We add the first k relationships of the sorted list X_i to R.
3. We return R for the function select_relationships(P_{ab}).

In this equation, n is the upper bound of the number of relationships for a class c_i^a that we want to test against.

3.3 Synthetic Taxonomy Generation

3.3.1 The Need for a Controlled Ground Truth

To evaluate our taxonomy generation methods, we need a reliable ground truth with known relationships between datasets. This presents a challenge, as most existing image classification datasets lack clear inter-dataset relationships:

- **ImageNet** [5, 33] uses WordNet's [9] hierarchical structure to organize classes. However, this strict hierarchy doesn't match our use case where we need to connect datasets with different class structures and partial overlaps.

- **Open Images** [26] contains approximately 9 million images with multiple labels per image generated by Google's Cloud Vision API[1]. This multi-label approach makes it difficult to determine a single class for each image, which is required for our evaluation. Additionally, since most labels were automatically generated, it doesn't provide the verified ground truth we need.

- **iNaturalist** [19] offers a detailed taxonomy of plant and animal species, but its domain-specific nature makes it unsuitable for developing a general-purpose evaluation framework.

3.3.2 Our Approach: Building Synthetic Datasets

Instead of relying on existing taxonomies, we developed a method to generate synthetic datasets with controlled relationships. Our approach:

1. Define a set of "atomic concepts" that serve as building blocks for classes
2. Create multiple domains by sampling these concepts to form classes
3. Calculate inter-domain relationships based on shared concepts

This method allows us to precisely control the taxonomy structure while creating realistic relationships between domains. To generate images for these synthetic classes, we can leverage existing datasets by treating each original class as an atomic concept.

3.3.3 Formal Definitions

We define our synthetic taxonomy framework on top of the definitions from section 3.1:

- **Atomic Concepts** $\mathcal{U} = \{1, 2, \ldots, n\}$: A set of atomic concepts will be a universe of concepts that make up the basis for our synthetic class generation.

- **Synthetic Class**: A class c_j^i will contain a subset of the atomic concepts from our universe: $c_j^i \subseteq \mathcal{U}$. To maintain disjoint class definitions, we ensure that $c_j^i \cap c_k^i = \emptyset$ for all $j \neq k$.

[1] https://cloud.google.com/vision

3.3.4 Randomized Domain Generation

To create realistic domains, we use normal distributions to sample the number of classes and concepts per class. This allows us to generate domains with varying sizes and complexities, mimicking different real-world datasets.

Parameter Sampling

We sample the number of classes per domain and the number of concepts per class from truncated normal distributions to ensure realistic variation while maintaining control. Since normal distributions are unbounded, we use a truncated version:

$$f(x|\mu,\sigma,a,b) = \begin{cases} \frac{\phi\left(\frac{x-\mu}{\sigma}\right)}{\sigma\left[\Phi\left(\frac{b-\mu}{\sigma}\right)-\Phi\left(\frac{a-\mu}{\sigma}\right)\right]} & \text{if } a \le x \le b \\ 0 & \text{otherwise} \end{cases}$$

Where:

- ϕ is the standard normal PDF
- Φ is the standard normal CDF
- a and b are lower and upper bounds

We implement this using SciPy's `truncnorm` module[2], handling SciPy's standardization of bounds internally:

$$X \sim \text{TruncNorm}(\mu, \sigma^2, a, b)$$

Domain Generation Algorithm

To generate a domain C_i, we follow these steps:

1. **Sample set size**: Determine how many concepts l to use for the domain:

$$l \sim \lfloor \text{TruncNorm}(\mu_{\text{concepts}}, \sigma^2_{\text{concepts}}, 1, n) \rceil$$

2. **Sample concept pool**: Randomly select l concepts from the universe $\mathcal{U}$:

$$P = \{a, b, c, ...\} \quad \text{where } a, b, c, ... \text{ are sampled without replacement from } \mathcal{U}$$

[2] https://docs.scipy.org/doc/scipy/reference/generated/scipy.stats.truncnorm.html

3. **Initialise domain**: $C_i = \{\}$

4. **Generate classes**: While concepts remain in the pool ($P \neq \emptyset$):

   a) Sample class size s_j:

   $$s_j \sim \lfloor \text{TruncNorm}(\mu_{\text{classes}}, \sigma^2_{\text{classes}}, 1, |P|) \rceil$$

   b) Form class c^i_j by selecting s_j concepts randomly from P

   c) Remove selected concepts: $P = P \setminus c^i_j$

   d) Add class to domain: $C_i = C_i \cup \{c^i_j\}$

This algorithm ensures that each concept is assigned to exactly one class within the domain, maintaining our disjointness constraint.

3.3.5 Modeling Cross-Domain Relationships

Once we've generated multiple domains, we need to model the relationships between them to create our ground truth.

Simulating Neural Network Predictions

Our taxonomy generation method assumes that neural network classifiers will predict related classes across domains with certain probabilities. To simulate this, we create "perfect" synthetic probabilities based on concept overlap.

Relationship Calculation

For any two domains C_A and C_B, we calculate the probability of classifying an instance of class c^A_i as class c^B_j using:

$$\begin{aligned} \text{NaiveProbability}(i,j) &= \frac{|c^A_i \cap c^B_j|}{|c^A_i|} \\ P_{i,j} &= \text{NaiveProbability}(i,j) + \frac{1 - \text{NaiveProbability}(i,j)}{|C_B|} \end{aligned} \tag{3.1}$$

Where:

- $\text{NaiveProbability}(i,j)$ is the proportion of concepts in class c^A_i that also appear in class c^B_j

- The second term distributes remaining probability mass evenly across all classes in domain C_B, simulating the behavior of a neural network when encountering concepts it hasn't seen before

A Concrete Example

To illustrate this approach, consider two domains:

- Domain A: $C_A = \{c_1^A = \{1, 2\}, c_2^A = \{3, 4\}\}$
- Domain B: $C_B = \{c_1^B = \{1, 2, 4\}, c_2^B = \{5, 6\}\}$

For the relationship $c_1^A \to c_1^B$:

- $\text{NaiveProbability}(1, 1) = \frac{|\{1,2\} \cap \{1,2,4\}|}{|\{1,2\}|} = \frac{2}{2} = 1$
- $P_{1,1} = 1 + \frac{1-1}{2} = 1$

For the relationship $c_2^A \to c_1^B$:

- $\text{NaiveProbability}(2, 1) = \frac{|\{3,4\} \cap \{1,2,4\}|}{|\{3,4\}|} = \frac{1}{2} = 0.5$
- $P_{2,1} = 0.5 + \frac{1-0.5}{2} = 0.5 + 0.25 = 0.75$

This example shows how our framework captures partial relationships between classes and how it simulates a perfect neural network classifier's behavior. The resulting probability prediction matrix between two domains can then be used to build a graph of relationships between classes, which can then be turned into a universal taxonomy using the methods described in section 3.2.

No-Prediction Classes

Some datasets have a special class that indicates that the model could not classify the image. For these "no-prediction" classes, we need to adapt the relationship probability calculation: Instead of distributing the remaining probability mass evenly across all classes, we simply ignore it and therefore only have the probability of the overlapping concepts.

3.4 Universal Taxonomy Algorithm

After constructing our initial graph structure from cross-domain predictions (as described in section 3.2), we now need to transform it into a universal taxonomy that merges classes from different datasets into universal classes where they share similar concepts.

3.4.1 Taxonomy Building Rules

1. **Isolated Node Rule**: For any domain class A that has no relationships (neither incoming nor outgoing edges), create a new universal class B and add the relationship $A \rightarrow B$. We also define the probability of the relationship's edge as 1 and the classes of the universal class as $\{A\}$.

   This ensures that all domain classes without relationships (which can be created by later rules) are still represented in the universal taxonomy.

2. **Bidirectional Relationship Rule**: When two classes have bidirectional relationships (A $\rightarrow$ B and B $\rightarrow$ A), they likely represent the same concept. We resolve this by creating a new universal class C and adding relationships $A \rightarrow C$ and $B \rightarrow C$ to the graph. The probability of the new relationships is set to the average of the bidirectional relationships and the classes of the universal class will be the two classes that were merged (or, if the two classes are universal classes themselves, the union of their classes).

3. **Transitive Cycle Rule**: If we have relationships A $\rightarrow$ B $\rightarrow$ C where A and C are in the same domain, we have a problem since classes within a domain are disjoint, which means that one of the relationships must be incorrect. We solve this by removing the relationship with the lower probability, thus breaking the cycle.

4. **Unilateral Relationship Rule**: A uniliteral relationship A $\rightarrow$ B indicates that the concepts of class A are a subset of the concepts of class B. We therefore create two new universal classes:

   - Class C, which contains both classes A and B and has incoming relationships from both classes with the probability of the uniliteral relationship. This universal class represents the union of the two classes.
   - Class D, which contains only class B and has a relationship from class B with a probability 1. This universal class represents the concepts of class B that are not in class A.

3.4.2 Difference to algorithm of Bevandic et al.

The taxonomy algorithm presented above is based on the work by Bevandic et al. [1], but adapted for image classification instead of semantic segmentation. Their original approach was designed to create universal taxonomies for multi-domain semantic segmentation by addressing the problem of incompatible labeling policies across datasets.

Original Algorithm

Bevandic et al. developed a procedure for constructing universal taxonomies that express dataset-specific labels as unions of disjoint universal visual concepts. Their algorithm operates on the principle that semantic classes can be viewed as sets of pixels, and uses three resolution rules to handle overlaps between classes from different datasets:

1. **Exact Match Rule**: If two classes match exactly across datasets, they are merged into a single universal class.
2. **Subset/Superset Rule**: If one class is a subset of another, the superset is decomposed into the subset plus a remainder class.
3. **Partial Overlap Rule**: If two classes partially overlap, they are split into three disjoint classes: the intersection, and the two remainders.

The algorithm iteratively applies these rules until all classes in the multiset are disjoint, creating a flat universal taxonomy that encompasses the entire semantic range of the dataset collection.

Our Modifications

Our approach adapts their methodology for image classification with several key modifications:

- **Classification vs. Segmentation**: While Bevandic et al. focused on pixel-level prediction for semantic segmentation, our method addresses image-level classification where each image has a single label from each dataset.
- **Probabilistic Relationships**: Instead of binary relationships between classes, we derive probabilities from the cross-domain predictions of our neural networks. This allows us to not only evaluate the quantity of relationships but also their quality e.g. useability for later classification tasks.
- **Flexible Relationship Selection**: We introduce multiple methods for selecting relevant relationships from probability matrices (naive thresholding, most common predictions, density thresholding, relationship hypothesis) and try to evaluate their performance on a synthetic ground truth.
- **Simplified Taxonomy Rules**: Our taxonomy building rules are adapted for the graph structure and focus on four main cases: isolated nodes, bidirectional relationships, transitive cycles, and unilateral relationships. They are very similar to the original rules, but simplified for our use case. For example, we do not need to handle the case of partial overlaps since we do not have pixel-level predictions.

- **Multi-domain Extension**: While the Bevandic et al. algorithm was designed for two datasets (and later iteratively adding more datasets), we directly support a multi-domain setting by constructing a single graph that captures relationships across all datasets. This allows us to build a universal taxonomy that connects multiple datasets in one go, rather than iteratively merging them.

These modifications allow our algorithm to work effectively in the image classification domain while maintaining the approach of the original work for handling incompatible taxonomies across multiple datasets.

3.5 Taxonomy Difference Metrics

Now that we have methods for generating a ground truth synthetic taxonomy, we need to define metrics to compare the predicted taxonomy against the ground truth. Comparison can happen at two points in our pipeline:

- **Universal Taxonomy Comparison**: Comparing the predicted universal taxonomy against the ground truth universal taxonomy. This is done after applying our universal taxonomy generation algorithm and allows us to evaluate the quality of the final taxonomy. However, the algorithm might change the scale of differences between our predicted and ground truth taxonomies (e.g. a unilateral vs. bidirectional relationship would be a small difference before the algorithm, but would result in a subset hypothesis with two universal classes vs. one universal class after the algorithm).

- **Relationship Graph Comparison**: Comparing the predicted graph of relationships between classes against the ground truth graph. This is done before converting the relationship graph into a universal taxonomy and allows us to evaluate the quality of the relationships between classes.

3.5.1 Constructing Adjacency Matrices

For our metrics, we first need to represent our intra-domain relationships as adjacency matrices. We concatinate every class from every domain into a single set of classes $C = \bigcup_{i=1}^{n} C_i$, where n is the number of domains. We then create an adjacency matrix $A \in [0,1]^{|C|\times|C|}$, where $A(i,j)$ is the relationship probability between classes c_i and c_j.

Additionally, we need to handle the case where a class has no relationships at all: Since these classes will later become a single universal class, we additionally create a self-loop for every class c_i without relationships, which is defined as $A(i,i) = 1$.

3.5.2 Edge Difference Ratio

Our first metric is the edge difference ratio (EDR), which measures the difference in edge weights between two relationship graphs G_1 and G_2. The metric is bounded between 0 and 1, where 0 indicates that the two graphs are identical and 1 indicates that the two graphs have no edges in common.

For two adjacency matrices A_1 and A_2 of graphs G_1 and G_2, we define the edge difference ratio as follows:

$$\mathrm{EDR}(G_1, G_2) = \frac{\sum_{i,j} |A_1(i,j) - A_2(i,j)|}{\sum_{i,j} \max(A_1(i,j), A_2(i,j))} \tag{3.2}$$

This definition captures the difference in edge weights between the two graphs, while normalizing it by the total edge weights in both graphs (without double counting edges).

Our EDR metric is similar to the Jaccard index [20] as well as the Tanimoto coefficient [36] when we consider the adjacency matrices as sets of edges. In contrast to these metrics, however, our EDR metric supports weighted edges, which allows us to respect the probabilities of relationships between classes.

3.5.3 Precision, Recall, and F1 Score

While the edge weights in our relationship graphs are important, every single edge (even with a very low probability) can create a new universal class and therefore change the universal taxonomy.

To account for this, we also define precision, recall, and F1 score metrics for the relationship graphs.

For two adjacency matrices A_1 and A_2 of graphs G_1 and G_2, we first create binarised versions of the matrices as B_1 and B_2, where $B_1(i,j) = 1$ if $A_1(i,j) > 0$ and $B_2(i,j) = 1$ if $A_2(i,j) > 0$.

Next, we compute the true positives, false positives, and false negatives as follows:

- **True Positives (TP)**: The number of edges that are present in both B_1 and B_2.
- **False Positives (FP)**: The number of edges that are present in B_1 but not in B_2.
- **False Negatives (FN)**: The number of edges that are present in B_2 but not in B_1.

Using these counts, we can then compute the precision, recall, and F1 score as follows:

- **Precision**: The ratio of true positives to the sum of true positives and false positives.
- **Recall**: The ratio of true positives to the sum of true positives and false negatives.
- **F1 Score**: The harmonic mean of precision and recall.

3.6 Universal Model Learning

After constructing our universal taxonomy, we need to train a model that can classify images using the universal classes rather than the original domain-specific classes. This requires creating a mapping system that converts between domain classes and universal classes, and adapting our learning algorithm to work with this unified representation.

3.6.1 Creation of Mapping Matrix from Taxonomy

To enable a neural network to learn from multiple domains simultaneously, we need to create a mapping matrix that converts domain class labels to universal class targets. This mapping is derived directly from the relationships in our universal taxonomy.

For each domain i with classes $C_i = \{c_1^i, c_2^i, \ldots, c_{k_i}^i\}$, we construct a mapping matrix $M_i \in \mathbb{R}^{|C_i| \times |U|}$, where U is the set of universal classes and $|U|$ is the number of universal classes.

Each element $M_i(j, u)$ represents the weight of the relationship between domain class c_j^i and universal class u. Formally, this weight is defined as:

$$M_i(j, u) = \begin{cases} w & \text{if there exists a relationship } c_j^i \to u \text{ with weight } w \\ 0 & \text{otherwise} \end{cases} \tag{3.3}$$

For converting domain class labels to universal class targets, we normalize each row of the matrix to ensure valid probability distributions:

$$\hat{M}_i(j, u) = \frac{M_i(j, u)}{\sum_{u' \in U} M_i(j, u')} \tag{3.4}$$

For example, if domain class c_1^0 has relationships to universal classes u_1 with weight 0.8 and u_2 with weight 0.4, the normalized probabilities would be:

$$\hat{M}_0(1, u_1) = \frac{0.8}{0.8 + 0.4} = \frac{2}{3}$$
$$\hat{M}_0(1, u_2) = \frac{0.4}{0.8 + 0.4} = \frac{1}{3}$$

3.6.2 Learning Function for Universal Model

Our universal model architecture consists of a standard convolutional neural network (e.g. ResNet) followed by a fully connected layer that outputs logits for each universal class. The key innovation lies in the loss function and target generation process.

Target Generation

For each training sample (x, c_j^i, i) where x is an image, c_j^i is the domain class label, and i is the domain identifier, we generate the universal class target using the normalized mapping matrix:

$$\mathbf{t} = \hat{M}_i[j, :] \tag{3.5}$$

where $\mathbf{t} \in [0, 1]^{|U|}$ is a probability distribution over universal classes.

Loss Function

Since our targets are probability distributions rather than one-hot vectors, we define our loss using the cross-entropy formula for discrete distributions. For model predictions $\mathbf{p} = \text{softmax}(\mathbf{z})$ where $\mathbf{z}$ are the logits, the loss is defined as:

$$\begin{aligned} H(\mathbf{t}, \mathbf{p}) &= -\sum_{u=1}^{|U|} \mathbf{t}(u) \log(\mathbf{p}(u)) \\ \mathscr{L}(\mathbf{t}, \mathbf{p}) &= H(\mathbf{t}, \mathbf{p}) \end{aligned} \tag{3.6}$$

This loss function encourages the model to produce predictions that match the target distribution derived from our universal taxonomy.

Inference and Evaluation

During inference, the model outputs a probability distribution over universal classes. To evaluate performance on the original domain classes, we need to convert these universal predictions back to domain-specific predictions using the transpose of the original (unnormalized) mapping matrix.

For universal predictions $\mathbf{p} \in [0, 1]^{|U|}$ and domain i, the domain class predictions are computed as:

$$\begin{aligned} \mathbf{d}_i &= M_i^T \mathbf{p} \\ \hat{c}_i &= \text{argmax}(\mathbf{d}_i) \end{aligned} \tag{3.7}$$

where $\mathbf{d}_i \in \mathbb{R}^{|C_i|}$ represents the predicted probabilities for each class in domain i and $\hat{c}_i$ is the final predicted class label.

Note that we use the original unnormalized matrix M_i (not $\hat{M}_i$) for this reverse mapping, as normalization would not change the final predictions and we can save computation during inference.

This approach allows our universal model to learn shared representations across domains represented by universal classes, trying to match the distribution over universal classes that lead to a target domain class.

4 Results & Discussion

4.1 Domain Models

4.1.1 Datasets

To begin our taxonomy generation, we first need datasets for training and evaluating our domain models:

- **Caltech-101 and Caltech-256** [13, 27]: The Caltech-101 dataset contains 101 object categories with 40 to 800 images per category, while Caltech-256 extends this to 256 categories with at least 80 images per category. Both datasets are widely used for image classification tasks[1]. Images are roughly 300x200 pixels and contain annotated outlines for each object, which we do not need for our purposes. Since the dataset has no predefined train/test split, we use an 80/10/10 split for training, validation, and testing.

- **CIFAR-100** [25]: The CIFAR-100 dataset contains 100 classes grouped into 20 superclasses, with 600 images per class. Each image is 32x32 pixels, significantly smaller than the Caltech datasets. This dataset is among the most popular for image classification tasks[2]. The dataset provides a train/test split of 50,000 training and 10,000 test images, which we further split by dividing the training set into 80% for training and 20% for validation.

- **Synthetic Datasets**: To have ground truth for our taxonomy generation, we create synthetic datasets based on Caltech-101 and CIFAR-100. These datasets evaluate our cross-domain relationship graph generation methods (see Section 3.2). We create synthetic datasets of varying sizes and complexity to evaluate how well our methods perform under different challenges.

[1] Over 500 open-access papers have cited the datasets, according to Papers with Code: https://paperswithcode.com/dataset/caltech-101 and https://paperswithcode.com/dataset/caltech-256

[2] Over 5000 open-access papers have cited the dataset, according to Papers with Code: https://paperswithcode.com/dataset/cifar-100

4.1.2 Training

Model Architecture

To begin training our domain models, we first define the model architecture. The ResNet architecture [16, 17] is a popular choice for image classification and has demonstrated strong performance across various datasets. It also has the advantage of being pre-trained on ImageNet [5, 33], saving us the effort of training from scratch. From the available ResNet sizes, we select the ResNet-50 architecture to meet our resource constraints.

We adapt the ResNet-50 architecture to our datasets by replacing the final fully connected layer with a funnel architecture that ends in an output layer matching the number of classes per dataset (see Figure 4.1).

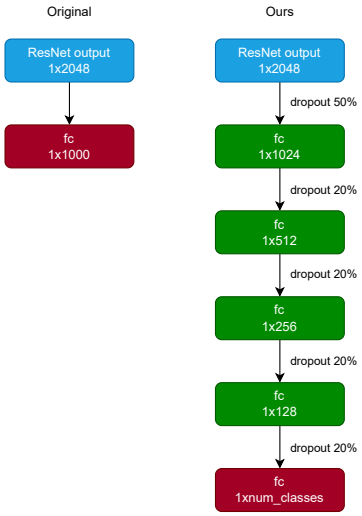

Figure 4.1: Our ResNet-50 architecture with a funnel layer for classification. Blue blocks represent the input from the ResNet-50 architecture, red blocks represent the final output layer, and green blocks represent our new funnel layers.

Training Procedure

In our initial training runs, we observed severe overfitting on the training data as shown in Figure 4.2. To mitigate this, we apply several regularization techniques:

- **Dropout** [18]: As shown in Figure 4.1, our fully connected layers contain dropout layers between them at rates of 0.5 and 0.2. Dropout is a regularization technique that randomly

sets a fraction of input units to zero during training, encouraging the model to learn more robust features and thereby reducing overfitting.

- **Data Augmentation**: We apply data augmentation techniques to our training data, including random cropping, horizontal flipping, random erasing, and color jittering. These techniques artificially increase our training dataset size and help the model generalize better by exposing it to a wider variety of input data.

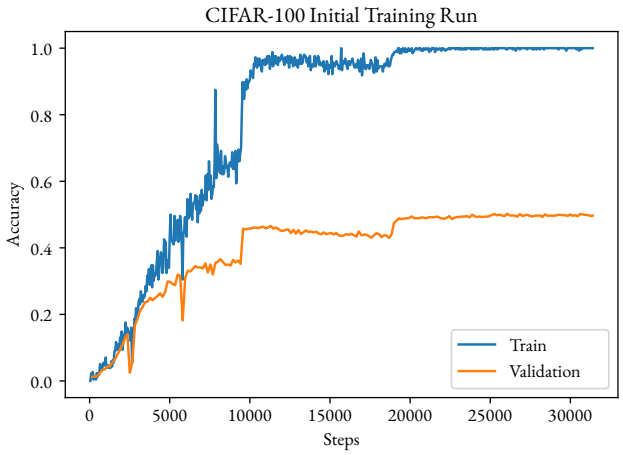

Figure 4.2: Overfitting on the CIFAR-100 dataset during training. The blue line represents the training accuracy, while the orange line represents the validation accuracy. The model overfits on the training data, resulting in a significant gap between the training and validation accuracy.

We now train our models on the Caltech-101, Caltech-256, and CIFAR-100 datasets (and their synthetic variants).

For the Caltech-101 and Caltech-256 datasets, we use the SGD optimizer [35] with a learning rate of 0.01, Nesterov momentum of 0.9, and weight decay of 0.0001, training all variants for 50 epochs. We also use a batch size of 64 for the datasets.

For the more complex CIFAR-100 dataset, we use the AdamW optimizer [28] with an initial learning rate of 0.001 and weight decay of 0.001. We train for 100 epochs with a multistep learning rate scheduler that reduces the learning rate by a factor of 0.1 at epochs 30, 60, and 80. For the smaller CIFAR-100 images we use a batch size of 256.

The training is performed on a single NVIDIA RTX 3070 GPU with 8GB of VRAM using the PyTorch Lightning framework [8]. The training process takes approximately 5 hours for the Caltech-101 and Caltech-256 synthetic dataset variants and approximately 3 hours for the CIFAR-100 synthetic dataset variants.

4.1.3 Model Performance

Synthetic Variants

For our evaluation of relationship selection methods (see Section 4.2.1), we need synthetic dataset variants to calculate evaluation metrics on.

We select the general-purpose Caltech-256 and CIFAR-100 datasets and create synthetic variants of these datasets:

- **Caltech-256 2-Domain Variant 1**: We create a basic 2-domain variant of the Caltech-256 dataset with parameters $\mu_{\text{concepts}} = 180$, $\sigma^2_{\text{concepts}} = 10$, $\mu_{\text{classes}} = 3$, and $\sigma^2_{\text{classes}} = 1$. The resulting relationship graph (before applying universal taxonomy algorithms) is shown in Figure 4.3a.

- **Caltech-256 2-Domain Variant 2**: We create a simpler 2-domain variant of the Caltech-256 dataset with parameters $\mu_{\text{concepts}} = 200$, $\sigma^2_{\text{concepts}} = 10$, $\mu_{\text{classes}} = 2$, and $\sigma^2_{\text{classes}} = 1$. This variant has fewer concepts per class and therefore fewer relationships between the classes, which might be more similar to simple real-world datasets. The resulting relationship graph (before applying universal taxonomy algorithms) is shown in Figure 4.3b.

- **Caltech-256 3-Domain Variant**: We create a more complex 3-domain variant of the Caltech-256 dataset with parameters $\mu_{\text{concepts}} = 180$, $\sigma^2_{\text{concepts}} = 10$, $\mu_{\text{classes}} = 5$, and $\sigma^2_{\text{classes}} = 1$. This variant has more concepts per class and therefore more relationships between the classes, which makes it more challenging for our relationship selection methods. These extreme numbers should be seen less as a realistic dataset and more as a stress test for our methods. The resulting relationship graph (before applying universal taxonomy algorithms) is shown in Figure 4.3c.

- **CIFAR-100 2-Domain Variant**: For the CIFAR-100 dataset, our 2-domain variant has parameters $\mu_{\text{concepts}} = 50$, $\sigma^2_{\text{concepts}} = 5$, $\mu_{\text{classes}} = 3$, and $\sigma^2_{\text{classes}} = 1$. In the Caltech-256 dataset variants we have used approximately 70% of the classes as concepts, while in the CIFAR-100 dataset variants we use approximately 50% of the classes as concepts. This results in a smaller, more manageable relationship graph that can be better manually inspected. The resulting relationship graph (before applying universal taxonomy algorithms) is shown in Figure 4.3d.

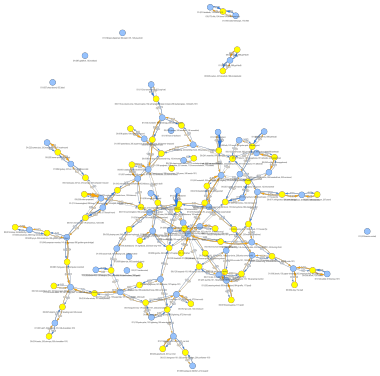

(a) Caltech-256 2-domain variant 1 ($\mu_{\text{concepts}} = 180$, $\sigma^2_{\text{concepts}} = 10$, $\mu_{\text{classes}} = 3$, $\sigma^2_{\text{classes}} = 1$)

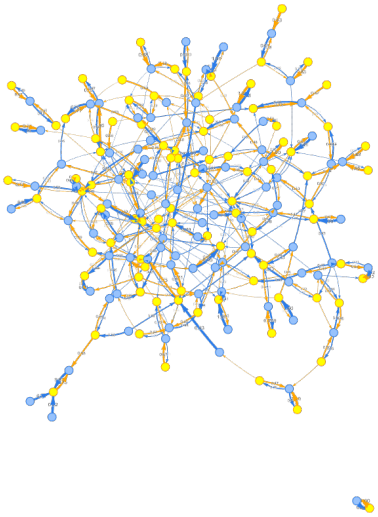

(b) Caltech-256 2-domain variant 2 ($\mu_{\text{concepts}} = 200$, $\sigma^2_{\text{concepts}} = 10$, $\mu_{\text{classes}} = 2$, $\sigma^2_{\text{classes}} = 1$)

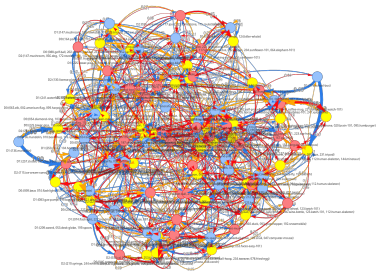

(c) Caltech-256 3-domain variant ($\mu_{\text{concepts}} = 180$, $\sigma^2_{\text{concepts}} = 10$, $\mu_{\text{classes}} = 5$, $\sigma^2_{\text{classes}} = 1$)

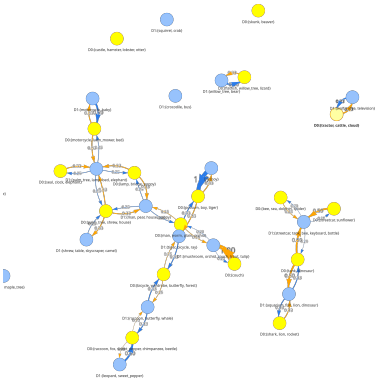

(d) CIFAR-100 2-domain variant ($\mu_{\text{concepts}} = 50$, $\sigma^2_{\text{concepts}} = 5$, $\mu_{\text{classes}} = 3$, $\sigma^2_{\text{classes}} = 1$)

Figure 4.3: Synthetic dataset variants showing their relationship graphs before applying universal taxonomy algorithms. The number of concepts and classes per concept are sampled from truncated normal distributions with the parameters shown in each subfigure caption.

Model Accuracy

Let us now take a look at the accuracy of our models trained on the synthetic dataset variants. We use checkpoints to save the model after each epoch and pick the model checkpoint with the lowest validation loss for our final evaluation.

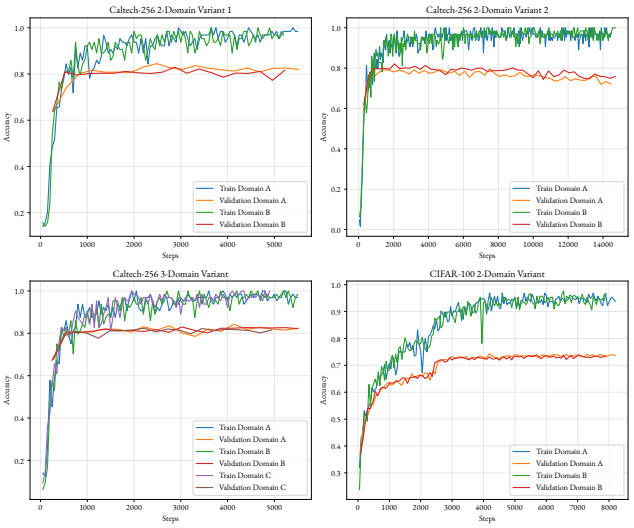

Figure 4.4: Accuracy curves for all synthetic dataset variants. Each subplot shows training and validation accuracy over training steps for all domains in that variant. The models achieve final training accuracies of approximately 0.96-0.98 and validation accuracies of approximately 0.73-0.83.

Table 4.1: Evaluation results on test sets. Models were checkpointed after every epoch and evaluated on the validation loss. The model with the lowest validation loss was selected for evaluation on the test set. Training time indicates the total duration from start to finish of model training.

Dataset Variant	Domain	Training Time	Accuracy
Caltech-256 2-Domain Variant 1	A	28m	0.83
Caltech-256 2-Domain Variant 1	B	25m	0.81
Caltech-256 2-Domain Variant 2	A	1h 12m	0.77
Caltech-256 2-Domain Variant 2	B	1h 12m	0.80
Caltech-256 3-Domain Variant	A	27m	0.84
Caltech-256 3-Domain Variant	B	26m	0.81
Caltech-256 3-Domain Variant	C	23m	0.81
CIFAR-100 2-Domain Variant	A	42m	0.77
CIFAR-100 2-Domain Variant	B	40m	0.75

We can see our final training runs in Figure 4.4. It can be observed that our overfitting mitigation techniques have worked sufficiently well, as our training and validation accuracy curves do not diverge significantly. We present the final model accuracies on the test sets in Table 4.1. Multiple things can be observed:

- All the models achieve an accuracy of around 0.8 on the test set, which is an average performance for these datasets. Our focus is not on achieving state-of-the-art performance, but rather on creating models suitable for our cross-domain prediction task. It should be

noted that a lower model accuracy will lead to worse performance in our relationship selection methods, but since we will compare the methods against each other using the same models, this should not be a problem.

- The CIFAR-100 variants have a slightly lower accuracy than the Caltech-256 variants, which is expected since the CIFAR-100 dataset has closely related classes categorised into superclasses, which make it harder for a model to distinguish between them.
- The number of concepts (i.e. classes) in the original dataset that get merged into a new class in the synthetic dataset variants does not seem to have a significant impact on the model accuracy: The Caltech-256 2-domain variant 2 has a $\mu_{\text{classes}} = 2$, while the Caltech-256 3-domain variant has a $\mu_{\text{classes}} = 5$, but the deviation in accuracy is negligible (≤ 0.05).

Now that we have sufficiently good domain models, we can use them to evaluate our relationship selection methods and generate taxonomies from the relationship graphs we create.

4.2 Taxonomy Generation

4.2.1 Relationship Selection Methods

Now that we have trained our domain models on the synthetic dataset variants, we can use them to evaluate our different relationship selection methods.

A good relationship selection method needs to be versatile enough to work on a range of different datasets with different characteristics:

- The number of relationships between classes can vary significantly, depending on the number of concepts and classes in the dataset. We therefore need a method that adapts to the probability distribution of the relationships instead of picking a fixed number of relationships.
- The number of classes in the dataset can also vary significantly, which means that some datasets might have classes with few, high probability relationships, while others might have classes with many, low probability relationships. Our method needs to be able to handle both cases and not be biased towards either.

Our edge difference ratio metric (see Section 3.5.2) is a good indicator of the overall accuracy of the relationship selection methods since it measures not only the number of relationships selected, but also the correctness (i.e. the edge weights) of the relationships.

However, since every selected relationship will later result in a node in the universal model, we need to give special attention to the correctness of the relationships selected. Therefore, we will

also evaluate the precision and recall of the selected relationships for each method on the synthetic dataset variants.

We will evalute every relationship selection method on every dataset variant by selecting the method parameters that yield the best edge difference ratio on that dataset variant.

Table 4.2: Best EDR results for relationship discovery methods. For each dataset variant and method, the parameter values that yielded the lowest Edge Difference Ratio (EDR) are shown along with the corresponding F1-score.

Dataset Variant	Method	EDR	F1-score	Parameter
Caltech-256 2-Domain Variant 1	MCFP	0.670	0.526	N/A
Caltech-256 2-Domain Variant 1	Naive Thresholding	**0.459**	**0.798**	0.15
Caltech-256 2-Domain Variant 1	Density Thresholding	0.508	0.662	0.70
Caltech-256 2-Domain Variant 1	Relationship Hypothesis	0.482	0.737	5
Caltech-256 2-Domain Variant 2	MCFP	0.557	0.625	N/A
Caltech-256 2-Domain Variant 2	Naive Thresholding	**0.402**	**0.834**	0.15
Caltech-256 2-Domain Variant 2	Density Thresholding	0.451	0.668	0.70
Caltech-256 2-Domain Variant 2	Relationship Hypothesis	0.429	0.774	4
Caltech-256 3-Domain Variant	MCFP	0.707	0.443	N/A
Caltech-256 3-Domain Variant	Naive Thresholding	**0.377**	**0.864**	0.10
Caltech-256 3-Domain Variant	Density Thresholding	0.420	0.740	0.75
Caltech-256 3-Domain Variant	Relationship Hypothesis	0.391	0.830	6
CIFAR-100 2-Domain Variant	MCFP	0.634	0.636	N/A
CIFAR-100 2-Domain Variant	Naive Thresholding	**0.525**	**0.770**	0.15
CIFAR-100 2-Domain Variant	Density Thresholding	0.562	0.688	0.40
CIFAR-100 2-Domain Variant	Relationship Hypothesis	0.534	0.595	4

When looking at the results in Table 4.2, we can observe two things:

- The naive thresholding method consistently performs best on all dataset variants, closely followed by the relationship hypothesis method. However, the threshold parameter for the naive thresholding method stays relatively consistent across the dataset variants (0.10 – 0.15), while the relationship hypothesis method has a much wider range of upper bounds (4 – 6).

- The original most common foreign prediction method from the Bevandic et al. paper [2] performs significantly worse than the other methods with an edge difference ratio of over 0.5 on all dataset variants. This was to be expected since our synthetic dataset variants rarely have classes with only a single outgoing relationship.

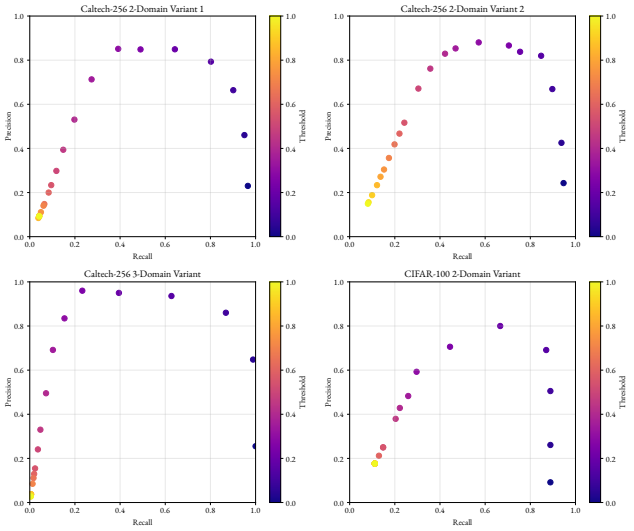

Figure 4.5: Precision and recall plot of the **naive thresholding method** for different thresholds on the Caltech-256 2-domain, Caltech-256 3-domain, and CIFAR-100 2-domain synthetic dataset variants.

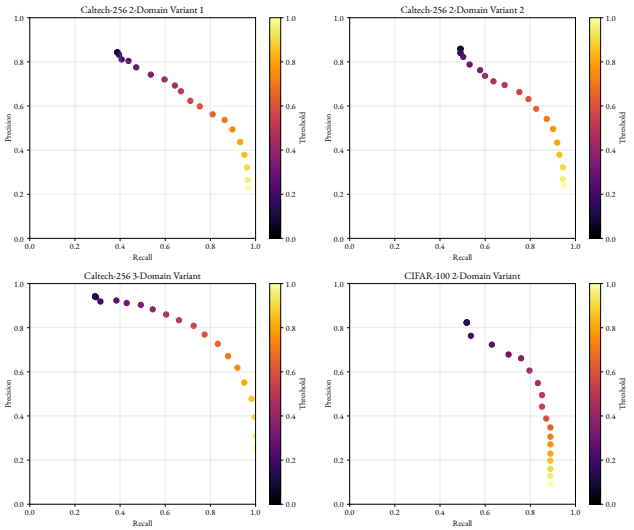

Figure 4.6: Precision and recall plot of the **density thresholding method** for different thresholds on the Caltech-256 2-domain, Caltech-256 3-domain, and CIFAR-100 2-domain synthetic dataset variants.

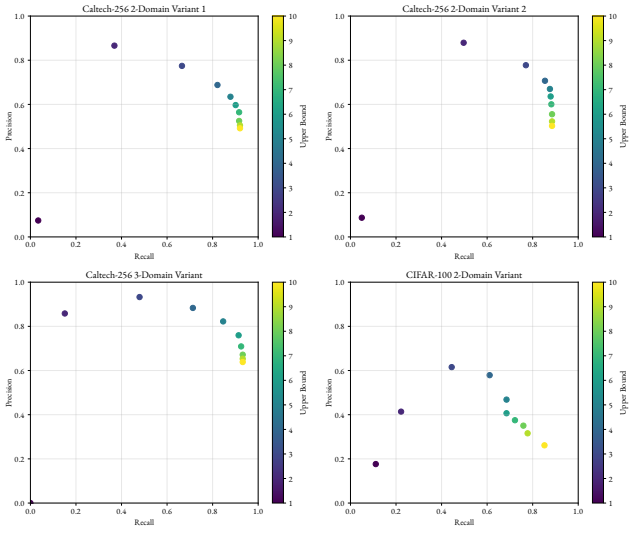

Figure 4.7: Precision and recall plot of the **hypothesis method** for different upper bounds on the Caltech-256 2-domain, Caltech-256 3-domain, and CIFAR-100 2-domain synthetic dataset variants.

Let us take a deeper look at each of the methods and their performance on the synthetic dataset variants using precision-recall curves for different parameters:

- The **naive thresholding method** (see Figure 4.5) performs well on all dataset variants, achieving a high precision and recall for thresholds between 0.10 and 0.15. The displayed precision-recall curves stay consistent across the dataset variants, which indicates that the method is robust for different dataset characteristics.

- The **density thresholding method** (see Figure 4.6) performs worse than the naive thresholding method, but still achieves good performance. Similar to the naive thresholding method, the CIFAR-100 dataset variant has a slightly lower precision and recall than the Caltech-256 dataset variants, which is expected since the CIFAR-100 dataset has more closely related classes that are difficult to distinguish.

- The **relationship hypothesis method** (see Figure 4.7) performs similar to the density thresholding method, but has a conspicuous drop for the CIFAR-100 dataset variant (prominently more so than the other methods). This is likely due to the fact that this method assumes that every true relationship has an equal probability, which is not the case for the CIFAR-100 dataset variant (where some merged classes, due to having similar concepts that are hard to distinguish, have a much higher probability than others).

When using our method on real-world datasets, we do not have a ground truth to adjust the parameters to. Therefore, we need a single parameter configuration for every method that works universally across all datasets.

We create a new evaluation on the dataset variants using the parameters that yield the best edge difference ratio averaged across all dataset variants. The results are shown in Table 4.3.

The best performing naive thresholding method achieves an edge difference ratio of 0.463 with a noticably higher recall (0.889) than precision (0.675). This means that while we hit almost 90% of the true relationships, we also select a lot of false relationships.

It can be observed that, for precsion, the mcfp method performs best with a precision of 0.865, which is expected since it only selects relationships that has the highest probability. However, this comes at the cost of a very low recall of 0.421 which ultimately results in a lower F1 score compared to the naive thresholding method.

We can conclude that, if you want to create singular high-confidence relationships, the mcfp method is the best choice (especially for single-hierarchy taxonomies). However, if you want to capture as many shared concepts as possible, the naive thresholding method is the best choice, closely followed by the relationship hypothesis method (maybe as a possible alternative if the naive thresholding method does not yield good results).

Table 4.3: Average performance metrics for relationship discovery methods with globally optimal parameters. Each method uses the parameter value that minimizes the average EDR across all dataset variants. Performance metrics are then averaged across all dataset variants using these optimal parameters.

Method	Parameter	EDR	Precision	Recall	F1-score
MCFP	N/A	0.642	**0.865**	0.421	0.557
Naive Thresholding	0.10	**0.463**	0.675	**0.889**	**0.760**
Density Thresholding	0.70	0.502	0.514	0.876	0.636
Relationship Hypothesis	4	0.472	0.714	0.750	0.727

However, these synthetic dataset variants might not be representative of real-world datasets, due to their shared image data as well as their "clean" relationships. But since our final goal is to create a universal model that works on multiple domains without separate head models, we can simply compare the universal model performance with our best candidate relationship selection methods (i.e. naive thresholding vs. most common foreign prediction).

Critique on Synthetic Dataset Variants

We can criticise our findings on the synthetic dataset variants by stating that the domains of the datasets are too similar and therefore do not represent a meaningful evaluation of our methods

for real-world datasets: Since the underlying images are the same, the models have a very high accuracy, which makes methods like naive thresholding very effective - even with a low threshold (which will not be the case for real-world datasets with different domains).

To verify or disprove our findings, we will try to create new, more realistic ground truth taxonomies:

- **WordNet Synsets:** The WordNet synsets [9, 40] represents a lexicon of english words with semantic relationships to each other. This allows us to create a taxonomy using WordNet with weighted relationships by calculating the Wu & Palmer similarity score (range 0-1) between two labels (i.e. WordNet words). The score measures the semantic similarity (1 means equal, 0 means no semantic relationship).

- **SVHN-MNIST:** MNIST [6] and SVHN [30] are both labelled datasets for digits. The MNIST dataset contains greyscale images of handwritten digits, while the SVHN dataset contains colour images of house numbers. This allows us to create a ground truth mapping between the two datasets by using the labels of the digits as the classes, while the domain of the images is different.

- **Domain-Shift Synthetic Datasets:** We can try to improve our synthetic dataset variants by applying different transformations to the images of the variants (e.g. greyscale, rotation, etc.). This will change the domain of the images while keeping the classes and relationships intact and therefore create a more "difficult" dataset for our methods.

WordNet Synsets

We test the usage of WordNet Synsets on the Caltech-101 and Caltech-256 datasets to build a relationship graph. It can be observed that the relationship weights (Wu & Palmer similarity scores) are very high (ranging between 0.8 and 1.0), even for weakly related synsets (e.g. between the Caltech256 class *snake* and the Caltech101 class *crocodile*, we observe a 0.88 relationship weight in both directions).

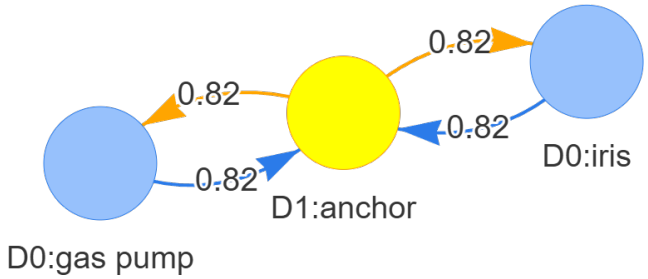

Figure 4.8: An example of a bad WordNet cluster in a relationship graph between Caltech256 and Caltech101. These false positives occur commonly and make WordNet unsuitable as a ground truth taxonomy.

Upon further observation, this problem turns out to be even more severe: WordNet's synsets build relations based on usage patterns in text corpora, which does not align with our visual relationships based on shared concepts and attributes. In Figure 4.8, we see a relationship cluster with the classes *gas pump*, *anchor* and *iris*. These words do not share any visual similarities or attributes, yet they are clustered together based on their textual relationships (we guess that *gas pump* and *anchor* are related through their usage in similar contexts like ships and maritime activities). Unfortunately upon manual inspection, these false positives occur frequently.

Since we try to build a ground truth taxonomy to evaluate relationship selection methods, these false positives can significantly skew the results and make WordNet unsuitable for our purposes.

SVHN-MNIST

Next, we try to use the SVHN and MNIST datasets to create a relationship graph. These datasets provide a special usability for our purposes, since the relationships between the classes can be manually defined. Also, since the datasets have a sufficiently shifted domain (i.e. drawn, greyscale images vs. real-world images of house numbers from different angles, lighting conditions, etc.), the differences are large enough to make the task of relationship selection more difficult and realistic.

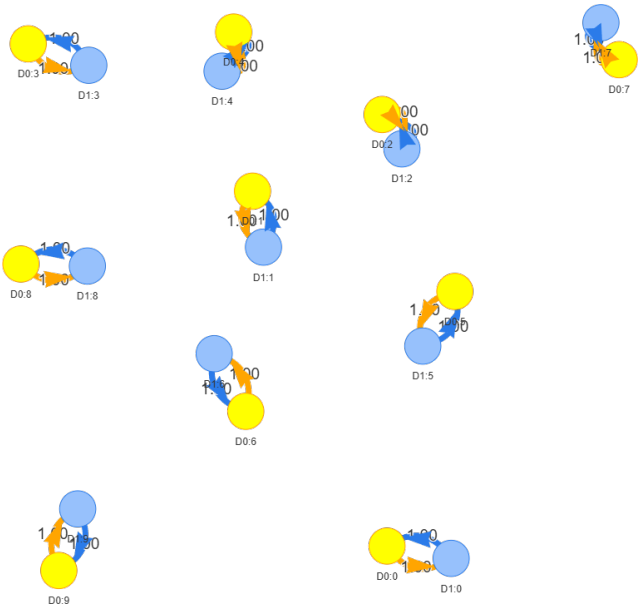

Figure 4.9: This figure shows the complete relationship graph between the SVHN and MNIST datasets. The relationships are unequivocal and straightforward, as the classes are identical across both datasets; however, they lack complexity.

In Figure 4.9, we can see the complete relationship graph between the SVHN and MNIST datasets. Every relationship is a simple connection between two classes with a weight of 1.0.

While we could rerun our relationship selection method evaluation on this taxonomy, we decide against this method upon further reflection:

- Real-world taxonomies will not be made up of single, isolated relationships with a weight of 1.0. Complex subsets, mismatches or overlaps between classes are completely missing.
- This taxonomy will have only ten universal classes, which makes the sample size too small to draw meaningful conclusions.
- Our previous datasets contained a wide range of general-purpose classes as well as more specific ones, which allowed for a more nuanced evaluation of our methods. This taxonomy will be limited to numbers.

Domain-Shift Synthetic Datasets

The main advantage of our synthetic dataset variants is their ability to create a proven correct ground truth taxonomy. Instead of trying to derive a ground truth using new, suboptimal methods, we instead try to fix the underlying issues with our existing method.

Our synthetic variants contain the same underlying images, which result in a near-perfect, unrealistic cross-domain model prediction accuracy. Due to this high model confidence, the best performing relationship selection methods are likely to be overly optimistic and therefore perform poorly in real-world scenarios where models will not be able to perform as well across domains.

Figure 4.10: Example images from the domain-shifted synthetic variants. We apply different transformations to the images of the original synthetic dataset to create two new domains. The first domain (Domain A) is a noisy greyscale variant, while the second domain (Domain B) is a rotated, blurry version of the original images, and the third domain (Domain C) has random erasings, shifted perspectives, and color jitter.

To mitigate this issue, we try to synthetically create a different domain for each variant by applying transforms to the underlying dataset images. An example subset of the domain-shifted images is shown in Figure 4.10: Using different transforms, the images appear in unique styles and distortions, synthetically changing their visual characteristics while retaining the same classes and relationships.

Table 4.4: Evaluation results on test sets for domain-shifted experiments. Models were trained with different domain shift transformations and checkpointed after every epoch. The model with the lowest validation loss was selected for evaluation on the test set. Training time indicates the total duration from start to finish of model training.

Dataset Variant	Domain	Training Time	Accuracy
Caltech-256 2-Domain Domain Shifted Variant 1	A	1h 44m	0.72
Caltech-256 2-Domain Domain Shifted Variant 1	B	2h 15m	0.76
Caltech-256 2-Domain Domain Shifted Variant 2	A	1h 51m	0.70
Caltech-256 2-Domain Domain Shifted Variant 2	B	2h 27m	0.75
Caltech-256 3-Domain Domain Shifted Variant	A	1h 42m	0.70
Caltech-256 3-Domain Domain Shifted Variant	B	2h 20m	0.75
Caltech-256 3-Domain Domain Shifted Variant	C	2h 22m	0.74
CIFAR-100 2-Domain Domain Shifted Variant	A	1h 1m	0.57
CIFAR-100 2-Domain Domain Shifted Variant	B	1h 39m	0.63

The training performance of these new domain-shifted models can be seen in Table 4.4. We can observe a 10% decrease in accuracy on the test data compared to the original synthetic dataset variants. This was to be expected due to the increased complexity of the domain-shifted tasks.

Table 4.5: Average performance metrics for relationship discovery methods with globally optimal parameters on domain-shifted experiments. Each method uses the parameter value that minimizes the average EDR across all domain-shifted dataset variants. Performance metrics are then averaged across all dataset variants using these optimal parameters.

Method	Parameter	EDR	Precision	Recall	F1-score
MCFP	N/A	0.842	**0.490**	0.226	0.305
Naive Thresholding	0.10	0.761	0.418	0.519	**0.450**
Density Thresholding	0.60	0.766	0.349	**0.582**	0.426
Relationship Hypothesis	5	**0.759**	0.390	0.543	0.444

When comparing the new averaged relationship method evaluation results in Table 4.5 to our original non-domain-shifted results in Table 4.3, we can observe significant differences:

- Our new best performing relationship selection method, based on averaged maximum EDR scores, changes from MCFP to the relationship hypothesis method.
- In general, all methods have a lower EDR score than their non-domain-shifted counterparts. This is a direct result of the decreased domain model accuracy and was to be expected.
- The MCFP method still has the highest relative precision with 0.49. If precision is more important than EDR for a high universal model accuracy will be evaluated in the universal model training section (see Section 4.3).

We will use the most promising relationship selection methods, MCFP and relationship hypothesis, for our universal model training. Our final evaluation will focus on the model accuracy of the trained universal Models built with the universal taxonomies of the two preselected relationship selection methods (using the selection method parameters that have the best EDR score).

4.2.2 Universal Taxonomy Generation

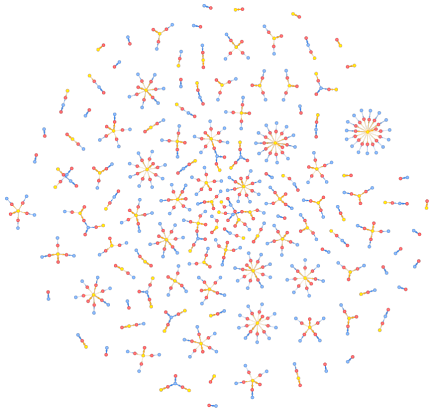

Figure 4.11: This figure shows the complete Caltech101-Caltech256 universal taxonomy. While most classes build smaller clusters build smaller clusters of 2-3 classes, some large clusters can be observed.

We now have our domain models trained and our relationship selection methods evaluated. In the next step, we run our universal taxonomy generation algorithm (see Section 3.4) on the Caltech-101 and Caltech-256 datasets. To make the results more interpretable, we will use the most common foreign prediction method to have a sparse relationship graph that is easier to look at (for our later universal model training, we will of course work with both the naive thresholding method and the most common foreign prediction method).

The overall universal taxonomy generated from the Caltech-101 and Caltech-256 datasets is shown in Figure 4.11. We can observe many smaller clusters of 2-3 classes which build from a single domain class in the Caltech-101 dataset and multiple domain classes in the Caltech-256 dataset (since the Caltech-256 dataset has more granular classes, this is to be expected).

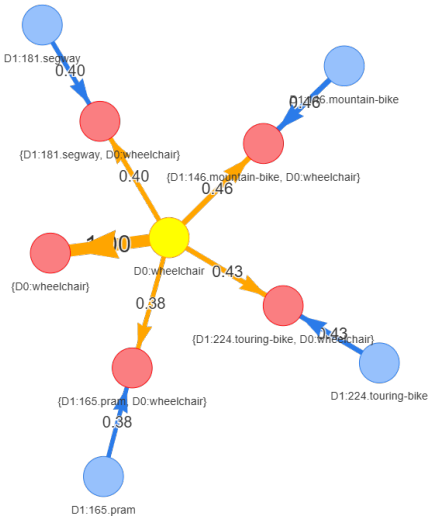

Figure 4.12: In the Caltech101-Caltech256 universal taxonomy, this cluster only contains vehicles. The universal classes created can be interpreted as sharing a common concept of "wheel".

An example of a "good" cluster is shown in Figure 4.12: This cluster centers around the Caltech101 class "wheelchair" and contains multiple Caltech256 classes that share the concept of "wheel" (e.g. "mountain bike", "segway", "touring bike", etc.). The universal classes between the Caltech101 and Caltech256 classes will provide a useful mapping for our universal model training.

Figure 4.13: This example in the Caltech101-Caltech256 universal taxonomy shows a wrong relationship cluster towards the Caltech101 class "binocular". Many of the Caltech256 classes do not have a suitable representation in the Caltech101 dataset and then connect to the Caltech101 class "binocular" instead.

However, we can also observe "bad" clusters in the universal taxonomy, such as the one shown in Figure 4.13: The Caltech101 class "binocular" is connected to multiple Caltech256 classes of a

variety of different concepts. While many of these classes do share concepts with binoculars (e.g. “sextant”, “telescope”, etc.), many of the Caltech256 classes in the cluster do not have an obvious connection to binoculars (e.g. “boxing glove”, “fire extinguisher”, etc.). Since it is likely that the Caltech256 dataset contains classes that do not have a suitable representation in the Caltech101 dataset, we “force” a relationship to a Caltech101 class by using the most common foreign prediction method. However, the incorrect relationships do have a low relationship weight which makes the error less severe for the universal model training.

Addressing these issues is a complex task, since a suitable threshold for the relationship weights depends on the individual composition of the datasets.

4.3 Universal Models

4.3.1 Training

Modifications to Baseline Architecture

Building upon the ResNet-50 architecture used for the individual domain models, we developed a `UniversalResNetModel` that incorporates several key modifications to enable multi-domain training through our universal taxonomy approach.

The most significant architectural change is the replacement of the standard classification head. While the baseline `ResNetModel` uses a multi-layer fully connected classifier with dropout regularization that outputs logits for domain-specific classes, the `UniversalResNetModel` employs a simplified two-layer fully connected head that outputs logits for universal classes:

- **Baseline classifier**: A 6-layer fully connected network with dropout (0.5, 0.2, 0.2, 0.2, 0.2) that progressively reduces dimensionality from ResNet features → 1024 → 512 → 256 → 128 → domain classes
- **Universal classifier**: A 2-layer fully connected network (ResNet features → 1024 → universal classes) without dropout regularization

The simplified architecture proved to be more effective in training runs vs. the more complex hopper + dropout architecture used in the baseline models.

Another crucial modification is the loss function: The baseline models use standard cross-entropy loss with one-hot encoded targets, while the universal model employs cross-entropy for discrete probability distributions for a loss function. This change accommodates the fact that domain classes may map to multiple universal classes with different weights, as determined by the taxonomy relationships (full explanation in Section 3.6).

Multi-Domain Training Procedure

Instead of training separate models on individual datasets, we create a new combined dataset that merges multiple datasets while preserving domain identity. Each training sample is augmented with a domain identifier, transforming the standard (`image`, `label`) pairs into (`image`, (`domain_id`, `label`)) tuples. This allows the model to handle samples from different datasets within the same batch (since we need to know the image domain to apply the correct target mapping).

During training experiments, the validation loss starts to increase again after a few epochs, indicating potential overfitting. However, the validation accuracy continues to improve, suggesting that the model is still learning useful features. To still use the best performing model checkpoint, we change checkpointing to monitor validation accuracy instead of validation loss.

This seemingly contradictory behavior of rising validation loss with rising validation accuracy can be explained by several factors:

- **Multi-target probability distributions**: Unlike standard classification with one-hot targets, our universal model uses discrete probability distributions as targets. The model may be learning to better predict the correct class ranks while becoming less confident about exact probability values, leading to higher cross-entropy loss but better top-1 accuracy.
- **Label smoothing**: The universal taxonomy creates implicit label smoothing effects where domain classes map to multiple universal classes with different weights. For perfect accuracy across all domains, it might not be possible to also hit the exact probability values, leading to higher loss *and* higher accuracy simultaneously while training.
- **Learning dynamics**: The model may be transitioning from overfitting to individual domain patterns toward learning more generalisable universal features, causing higher loss when switching between phases of learning.

As a final note on the training procedure, we rescale the CIFAR-100 images to match the size of the other datasets (224x224 pixels), so that we can process all images uniformly in the same model architecture.

4.3.2 Performance

On the Caltech-101 + Caltech-256 multi-domain dataset, we train universal models on all four relationship selection methods. Additionally, we introduce a *MCFP binary* relationship selection method, which uses a fixed weight of 1 for every relationship. This additional variant mimics the original MCFP method by Bevandic et al. [2] and serves as an additional baseline for comparison.

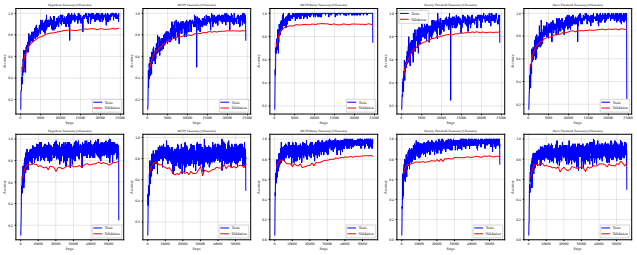

Figure 4.14: Training curves for universal models using both hypothesis and MCFP taxonomies on the multi-domain Caltech-101 + Caltech-256 dataset. Both models show stable convergence with the hypothesis taxonomy achieving slightly better performance.

When looking at the training curves in Figure 4.14, we observe slight overfitting in the later training steps, but overall the models show stable convergence. It is interesting to note that some rapid, short fluctuations occur in the training curves which get quickly mitigated. This could indicate exploding gradients or other instabilities during training, but since they are short-lived and do not affect the overall convergence, we can conclude that the training process is robust.

Table 4.6: Baseline ResNet model performance on individual datasets. These single-domain models serve as reference points for evaluating the universal models. Every baseline model was trained for 50 epochs.

Dataset	Architecture	Optimizer	Test Accuracy
Caltech-101	ResNet-50	SGD	91.81
Caltech-256	ResNet-50	AdamW	69.48
CIFAR-100	ResNet-152	AdamW	60.48

We compare the performance of the universal models with baseline models (models using the same architecture and training conditions, but trained for a single domain). Our baseline model performances are shown in Table 4.6: We use the same ResNet-50 architecture that we use in the universal models (except for CIFAR-100, where we achieve an unsuitable test accuracy of below 50% when using ResNet-50, so we decided to use ResNet-152). The baseline models were also used as domain models to create the cross-prediction mappings for the universal taxonomies that the universal models are using.

The final evaluation results of our universal models are shown in Table 4.7 and Table 4.8. All versions use ResNet-50 with AdamW optimizers and train for 50 epochs.

First of all, we notice that the domain models get outperformed by most of the universal models, with some relationship selection methods (e.g. density thresholding) achieving significantly better results than the baselines across all taxonomies and datasets.

Table 4.7: Universal model evaluation results for two-domain models trained on Caltech-101 + Caltech-256. Models were evaluated on the test sets of the individual domains. Domain accuracy values show performance differences compared to single-domain baseline models (see Table 4.6). Best results per column are shown in bold. All accuracy values are shown as percentages. Density Threshold models use parameter 0.6, Naive Threshold models use parameter 0.1.

Taxonomy	Caltech-101	Caltech-256	Avg
Hypothesis	91.81 (+0.00)	82.84 (+13.36)	87.33
MCFP	91.23 (-0.58)	80.75 (+11.27)	85.99
MCFP Binary	92.73 (+0.92)	**89.71 (+20.23)**	**91.22**
Density Threshold	92.96 (+1.15)	81.54 (+12.06)	87.25
Naive Threshold	**93.19 (+1.38)**	82.25 (+12.77)	87.72

Table 4.8: Universal model evaluation results for three-domain models trained on Caltech-101 + Caltech-256 + CIFAR-100. Models were evaluated on the test sets of the individual domains. Domain accuracy values show performance differences compared to single-domain baseline models (see Table 4.6). Best results per column are shown in bold. All accuracy values are shown as percentages. Density Threshold models use parameter 0.6, Naive Threshold models use parameter 0.1.

Taxonomy	Caltech-101	Caltech-256	CIFAR-100	Avg
Hypothesis	68.74 (-23.07)	58.17 (-11.31)	69.03 (+8.55)	65.31
MCFP	83.28 (-8.53)	76.50 (+7.02)	76.10 (+15.62)	78.63
MCFP Binary	94.58 (+2.77)	85.13 (+15.65)	82.71 (+22.23)	**87.47**
Density Threshold	95.39 (+3.58)	83.53 (+14.05)	**83.14 (+22.66)**	87.35
Naive Threshold	**95.50 (+3.69)**	**85.36 (+15.88)**	72.56 (+12.08)	84.47

Our comparison between the original MCFP binary relationship selection method and our proposed new methods is quite ambiguous: While the MCFP binary method achieves best overall average performance across the used individual datasets for both taxonomies, other relationship selection methods outperform it on specific datasets.

It is also important to note that no single relationship selection method consistently outperforms the others across all datasets and taxonomies. We have multiple possible explanations for this phenomenon:

- Our relationship selection parameters were badly chosen and do not represent a global optimum. Our synthetic taxonomies may not adequately capture the complexities of the real-world relationships present in the data, or, the metric of edge difference ratio may not be as relevant for universal model generalization as we initially thought. A sensible approach to address this issue would be to use a grid search by training multiple universal models with different relationship selection parameters and selecting the best performing one. How-

ever, since this would require significant computation resources, we leave this as future work.

- It might not be possible to find a single, universally optimal relationship selection method. Different datasets and taxonomies may require different approaches to relationship selection to achieve the best performance. A possible solution could be to start a reduced test run to preselect promising relationship selection parameters before conducting a full-scale training run. However, this would need to be explored thoroughly in future work.

We can conclude that much further work is needed to explore the relationship selection methods and their impact on universal model performance. There is also no clear correlation between our relationship selection metrics (see Table 4.5) and the universal model performance.

It needs to be investigated what factors contribute to the observed discrepancies between the relationship selection metrics and the universal model performance (e.g. dataset characteristics, number of datasets used in the taxonomies, etc.).

4.3.3 Feature Visualization

As a final evaluation of our different universal models, we will visualize the final output layer representations using t-SNE [29].

We choose t-SNE as our dimensionality reduction technique because it preserved local structure information which we want to inspect, making it better suited than simpler, linear techniques like PCA [12].

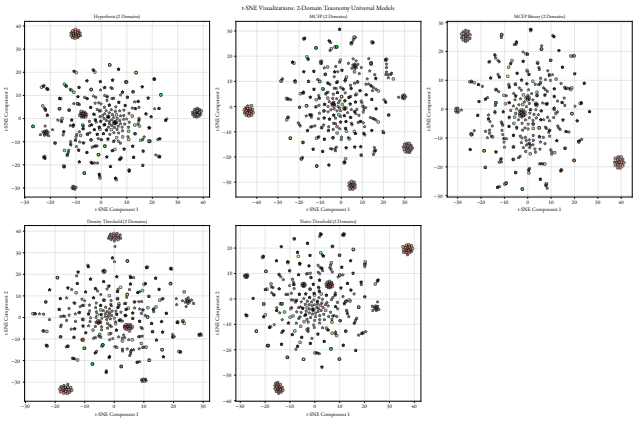

Figure 4.15: t-SNE visualization of the final output layer representations for the universal models on the Caltech-101 + Caltech-256 taxonomies. Classes are represented through colours, marker shapes indicate the dataset. Circles represent the Caltech-101 dataset, stars represent the Caltech-256 dataset.

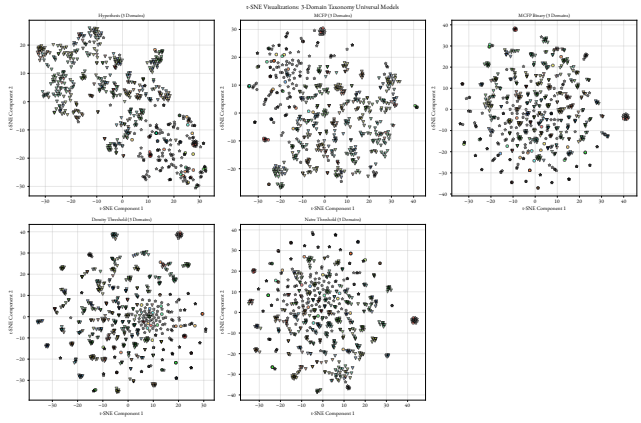

Figure 4.16: t-SNE visualization of the final output layer representations for the universal models on the Caltech-101 + Caltech-256 + CIFAR-100 taxonomies. Classes are represented through colours, marker shapes indicate the dataset. Circles represent the Caltech-101 dataset, stars represent the Caltech-256 dataset, and triangles represent the CIFAR-100 dataset.

We see the t-SNE visualizations in Figure 4.15 and Figure 4.16. For the 2-domain taxonomy (Caltech-101 + Caltech-256), we observe 2-3 clusters forming, possibly the clutter clusters we observed in Figure 4.13.

For both the 2-domain and the 3-domain taxonomy, we observe many smaller clusters with a mix of classes from different datasets. These clusters indicate potential overlaps and shared features between the datasets, highlighting the advantages of using a universal taxonomy to capture these relationships.

In other examples, we can observe a separation of classes from different datasets, possibly for classes that do not share any concepts or features with other datasets.

We can conclude that the feature space of our universal models is sufficiently rich to capture the underlying relationships between different datasets and classes. The structural differences that are noticable in the t-SNE visualizations between the different relationship selection methods support the need for further investigation into their impact on model performance.

5 Conclusion

In this thesis, we addressed the challenge of training universal image classification models across multiple datasets with discrepant taxonomies. Our research focused on developing automated methods for creating universal taxonomies that map relationships between classes across different domains from cross-domain predictions, enabling unified model training without task-specific adaptations (in contrast to popular multi-head architectures).

5.1 Summary of Contributions

We explored various methods for addressing multi-dataset image classification challenges, building on existing work in taxonomy learning and label alignment.

5.1.1 Automated Taxonomy Generation Framework

We developed a comprehensive framework for automatically generating universal taxonomies from multiple image classification datasets. Building upon the method of Bevandic et al. [1, 2], we adapted their semantic segmentation approach for image classification by:

- Creating a cross-domain graph generation algorithm that uses neural network predictions to identify relationships between classes from different datasets automatically without manual intervention.
- Developing four relationship selection methods (naive thresholding, most common foreign predictions, density thresholding, and relationship hypothesis) to filter relevant connections from noisy cross-domain predictions.
- Implementing universal taxonomy building rules that resolve conflicts between domains and create coherent universal class structures.

5.1.2 Synthetic Dataset Generation for Evaluation

Evaluation of cross-domain relationship graphs is challenging due to the lack of ground truth data. To address this, we created a novel synthetic dataset generation framework that:

- Defines atomic concepts as building blocks for synthetic classes.
- Uses probabilistic sampling to create realistic domain variations with controlled complexity, providing a flexible framework to test a range of different scenarios.
- Generates ground truth relationships based on concept overlap, allowing precise evaluation of taxonomy generation methods.
- Includes domain-shifted variants to simulate realistic cross-domain challenges.

This synthetic framework provided crucial ground truth data for evaluating relationship selection methods; something existing real-world datasets could not offer reliably. The framework is built modularly to enable easy extension and adaptation for future research.

5.1.3 Comprehensive Evaluation Metrics

We introduced specialized metrics for comparing predicted and ground truth taxonomies:

- Edge Difference Ratio (EDR) to measure overall relationship accuracy while considering edge weights
- Precision, recall, and F1 scores adapted for relationship graphs

5.1.4 Universal Model Learning Architecture

We designed and implemented a universal learning system that:

- Creates mapping matrices from universal taxonomies to convert domain-specific labels into universal class targets.
- Uses discrete probability distributions as training targets instead of traditional one-hot encodings.
- Employs cross-entropy loss for probability distributions to handle multi-target relationships.
- Enables inference across multiple domains through a single unified model.

While this learning system is implemented for the ResNet architecture, it can be easily adapted to other architectures, making it reusable across different model types.

5.2 Key Findings

Our experimental evaluation on both synthetic and real-world datasets revealed several important insights about the effectiveness of our approach:

5.2.1 Universal Model Effectiveness

Our universal models demonstrated promising results, consistently outperforming domain-specific baseline models on individual datasets. We conclude that leveraging multi-domain training approaches provides significant benefits compared to traditional single-domain training.

Unlike existing work, our approach can train on any number of datasets simultaneously, making it highly scalable and adaptable to various multi-domain scenarios.

5.2.2 Feature Space Representation Quality

t-SNE visualization of universal model representations revealed meaningful clustering patterns that reflected the underlying taxonomy structure. We observed both multi-domain and domain-specific clusters, indicating that the model successfully learned to identify shared concepts across different datasets and domain-specific classes.

5.2.3 Synthetic Evaluation Framework Validation

The synthetic dataset generation framework proved essential for reliable evaluation of taxonomy generation methods. The framework successfully provided ground truth data that was previously unavailable for real-world datasets, enabling precise quantitative assessment of relationship selection approaches.

5.3 Limitations and Challenges

Despite promising results, our work encountered several limitations that highlight areas requiring further investigation:

5.3.1 Relationship Selection Method Inconsistency

No single relationship selection method consistently outperformed others across all scenarios. Performance varied significantly depending on specific dataset combinations and domain characteristics, indicating that current approaches lack robustness across diverse scenarios.

5.3.2 Parameter Sensitivity

Relationship selection methods showed significant sensitivity to parameter choices, and no single parameter configuration worked optimally across all dataset combinations. This parameter dependency limits practical applicability without extensive hyperparameter tuning for each new dataset combination.

5.3.3 Evaluation Ground Truth Limitations

Creating reliable ground truth taxonomies for real-world datasets proved challenging. WordNet-based approaches suffered from semantic relationships that didn't align with visual similarities, while simple datasets like SVHN-MNIST lacked the complexity needed for meaningful evaluation.

Our synthetic dataset generation framework, while a significant improvement, still faced challenges in perfectly capturing the complexities of real-world scenarios. The domain-shifted synthetic datasets better reflected real-world challenges than original variants but remained imperfect proxies for actual cross-domain relationships.

5.4 Future Work

Based on our findings and limitations, several promising research directions emerge:

5.4.1 Adaptive Relationship Selection

Future work should investigate hybrid relationship selection methods that can adapt to dataset characteristics and automatically adjust parameters based on domain properties. This could address current inconsistency issues and improve robustness across diverse scenarios.

5.4.2 Enhanced Ground Truth Generation

Research into creating more realistic ground truth datasets that better capture the complexities of real-world cross-domain relationships is needed. This could involve improved synthetic data generation techniques or semi-supervised approaches that leverage human expertise more effectively.

5.4.3 Comprehensive Universal Taxonomies

Training universal models on single, comprehensive taxonomies that span multiple datasets (both general-purpose and specialized) represents an interesting avenue for future research. Such an approach could potentially unlock the full benefits of large-scale multi-domain learning by training

on a huge amount of data from diverse sources simultaneously and automatically discovering relationships between all classes.

5.5 Final Remarks

This thesis presented a comprehensive approach to multi-dataset image classification through automated universal taxonomy generation. Our work demonstrates that it is possible to automatically discover meaningful relationships between classes across different domains and leverage these relationships to train effective universal models.

The combination of our automated taxonomy generation framework, synthetic evaluation methodology, and universal learning architecture provides a solid foundation for future research in cross-domain image classification. While challenges remain, particularly in relationship selection consistency and ground truth evaluation, our results show clear benefits of multi-domain training approaches over traditional single-domain methods.

The scalability and adaptability of our approach, combined with its ability to work with any number of datasets simultaneously, positions it as a valuable contribution to multi-domain machine learning. As available image classification datasets continue to grow, methods like ours will become increasingly important for leveraging the full potential of diverse visual data sources.

Bibliography

1. P. Bevandić, M. Oršić, I. Grubišić, J. Šarić, and S. Šegvić. "Weakly supervised training of universal visual concepts for multi-domain semantic segmentation". *International Journal of Computer Vision* 132:7, 2024, pp. 2450–2472. ISSN: 0920-5691, 1573-1405. DOI: 10.1007/s11263-024-01986-z. arXiv: 2212.10340[cs]. URL: http://arxiv.org/abs/2212.10340 (visited on 03/19/2025).

2. P. Bevandić and S. Šegvić. *Automatic universal taxonomies for multi-domain semantic segmentation*. 26, 2022. DOI: 10.48550/arXiv.2207.08445. arXiv: 2207.08445[cs]. URL: http://arxiv.org/abs/2207.08445 (visited on 04/21/2025).

3. G. Bordea, E. Lefever, and P. Buitelaar. "SemEval-2016 Task 13: Taxonomy Extraction Evaluation (TExEval-2)". In: *Proceedings of the 10th International Workshop on Semantic Evaluation (SemEval-2016)*. SemEval 2016. Ed. by S. Bethard, M. Carpuat, D. Cer, D. Jurgens, P. Nakov, and T. Zesch. Association for Computational Linguistics, San Diego, California, 2016, pp. 1081–1091. DOI: 10.18653/v1/S16-1168. URL: https://aclanthology.org/S16-1168/ (visited on 08/17/2025).

4. B. Chen, F. Yi, and D. Varró. *Prompting or Fine-tuning? A Comparative Study of Large Language Models for Taxonomy Construction*. 4, 2023. DOI: 10.48550/arXiv.2309.01715. arXiv: 2309.01715[cs]. URL: http://arxiv.org/abs/2309.01715 (visited on 08/17/2025).

5. J. Deng, W. Dong, R. Socher, L.-J. Li, K. Li, and L. Fei-Fei. "ImageNet: A Large-Scale Hierarchical Image Database". In: *CVPR09*. 2009.

6. L. Deng. "The mnist database of handwritten digit images for machine learning research". *IEEE Signal Processing Magazine* 29:6, 2012, pp. 141–142.

7. J. Donahue, Y. Jia, O. Vinyals, J. Hoffman, N. Zhang, E. Tzeng, and T. Darrell. "DeCAF: A Deep Convolutional Activation Feature for Generic Visual Recognition". In: *Proceedings of the 31st International Conference on Machine Learning*. Ed. by E. P. Xing and T. Jebara. Vol. 32. Proceedings of Machine Learning Research. PMLR, Bejing, China, 22, 2014, pp. 647–655. URL: https://proceedings.mlr.press/v32/donahue14.html.

8. W. Falcon and The PyTorch Lightning team. *PyTorch Lightning*. Version 1.4. 2019. DOI: 10.5281/zenodo.3828935. URL: https://github.com/Lightning-AI/lightning.

9. C. Fellbaum. *WordNet: An Electronic Lexical Database*. The MIT Press, 1998. ISBN: 9780262272551. DOI: 10.7551/mitpress/7287.001.0001. URL: https://doi.org/10.7551/mitpress/7287.001.0001.

10. D. Firmani, S. Galhotra, B. Saha, and D. Srivastava. "Building Taxonomies with Triplet Queries". In: Sistemi Evoluti per Basi di Dati. 2024. URL: https://www.semanticscholar.org/paper/Building-Taxonomies-with-Triplet-Queries-Firmani-Galhotra/91e314dd5df505d036aa49ddeb3562551770afb6 (visited on 08/17/2025).

11. Y. Ganin, E. Ustinova, H. Ajakan, P. Germain, H. Larochelle, F. Laviolette, M. Marchand, and V. Lempitsky. "Domain-adversarial training of neural networks". *J. Mach. Learn. Res.* 17:1, 2016, pp. 2096–2030. ISSN: 1532-4435.

12. F. L. Gewers, G. R. Ferreira, H. F. D. Arruda, F. N. Silva, C. H. Comin, D. R. Amancio, and L. D. F. Costa. "Principal Component Analysis: A Natural Approach to Data Exploration". *ACM Comput. Surv.* 54:4, 2021. ISSN: 0360-0300. DOI: 10.1145/3447755. URL: https://doi.org/10.1145/3447755.

13. G. Griffin, A. Holub, and P. Perona. *Caltech 256*. 6, 2022. DOI: 10.22002/D1.20087. URL: https://data.caltech.edu/records/20087 (visited on 06/20/2025).

14. M. Gunn, D. Park, and N. Kamath. *Creating a Fine Grained Entity Type Taxonomy Using LLMs*. 19, 2024. DOI: 10.48550/arXiv.2402.12557. arXiv: 2402.12557[cs]. URL: http://arxiv.org/abs/2402.12557 (visited on 08/17/2025).

15. K. He, R. Girshick, and P. Dollar. "Rethinking ImageNet Pre-Training". In: *2019 IEEE/CVF International Conference on Computer Vision (ICCV)*. 2019, pp. 4917–4926. DOI: 10.1109/ICCV.2019.00502.

16. K. He, X. Zhang, S. Ren, and J. Sun. *Deep Residual Learning for Image Recognition*. 2015. DOI: 10.48550/ARXIV.1512.03385. URL: https://arxiv.org/abs/1512.03385 (visited on 06/20/2025).

17. K. He, X. Zhang, S. Ren, and J. Sun. "Identity Mappings in Deep Residual Networks". *arXiv preprint arXiv:1603.05027*, 2016.

18. G. E. Hinton, N. Srivastava, A. Krizhevsky, I. Sutskever, and R. R. Salakhutdinov. *Improving neural networks by preventing co-adaptation of feature detectors*. 2012. DOI: 10.48550/ARXIV.1207.0580. URL: https://arxiv.org/abs/1207.0580 (visited on 06/21/2025).

19. G. V. Horn, O. M. Aodha, Y. Song, Y. Cui, C. Sun, A. Shepard, H. Adam, P. Perona, and S. Belongie. *The iNaturalist Species Classification and Detection Dataset*. 10, 2018. DOI: 10.48550/arXiv.1707.06642. arXiv: 1707.06642[cs]. URL: http://arxiv.org/abs/1707.06642 (visited on 05/03/2025).

20. P. Jaccard. "The Distribution of the Flora in the Alpine Zone." *New Phytologist* 11:2, 1912, pp. 37–50. ISSN: 1469-8137. DOI: 10.1111/j.1469-8137.1912.tb05611.x. URL: https://onlinelibrary.wiley.com/doi/abs/10.1111/j.1469-8137.1912.tb05611.x (visited on 06/01/2025).

21. D. Jurgens and M. T. Pilehvar. "SemEval-2016 Task 14: Semantic Taxonomy Enrichment". In: *Proceedings of the 10th International Workshop on Semantic Evaluation (SemEval-2016)*. SemEval 2016. Ed. by S. Bethard, M. Carpuat, D. Cer, D. Jurgens, P. Nakov, and T. Zesch. Association for Computational Linguistics, San Diego, California, 2016, pp. 1092–1102. DOI: 10.18653/v1/S16-1169. URL: https://aclanthology.org/S16-1169/ (visited on 08/17/2025).

22. P. Kargupta, N. Zhang, Y. Zhang, R. Zhang, P. Mitra, and J. Han. *TaxoAdapt: Aligning LLM-Based Multidimensional Taxonomy Construction to Evolving Research Corpora*. version: 1. 12, 2025. DOI: 10.48550/arXiv.2506.10737. arXiv: 2506.10737[cs]. URL: http://arxiv.org/abs/2506.10737 (visited on 08/17/2025).

23. A. Kolesnikov, L. Beyer, X. Zhai, J. Puigcerver, J. Yung, S. Gelly, and N. Houlsby. *Big Transfer (BiT): General Visual Representation Learning*. version: 3. 5, 2020. DOI: 10.48550/arXiv.1912.11370. arXiv: 1912.11370[cs]. URL: http://arxiv.org/abs/1912.11370 (visited on 03/31/2025).

24. S. Kornblith, J. Shlens, and Q. V. Le. "Do Better ImageNet Models Transfer Better?" In: *2019 IEEE/CVF Conference on Computer Vision and Pattern Recognition (CVPR)*. 2019, pp. 2656–2666. DOI: 10.1109/CVPR.2019.00277.

25. A. Krizhevsky and G. Hinton. "Learning multiple layers of features from tiny images", 2009. URL: http://www.cs.utoronto.ca/~kriz/learning-features-2009-TR.pdf (visited on 03/19/2025).

26. A. Kuznetsova, H. Rom, N. Alldrin, J. Uijlings, I. Krasin, J. Pont-Tuset, S. Kamali, S. Popov, M. Malloci, A. Kolesnikov, T. Duerig, and V. Ferrari. "The Open Images Dataset V4: Unified image classification, object detection, and visual relationship detection at scale". *IJCV*, 2020.

27. F.-F. Li, M. Andreeto, M. Ranzato, and P. Perona. *Caltech 101*. Version 1.0. 6, 2022. DOI: 10.22002/D1.20086. URL: https://data.caltech.edu/records/20086 (visited on 03/19/2025).

28. I. Loshchilov and F. Hutter. *Decoupled Weight Decay Regularization*. 2017. DOI: 10.48550/ARXIV.1711.05101. URL: https://arxiv.org/abs/1711.05101 (visited on 06/21/2025).

29. L. v. d. Maaten and G. Hinton. "Visualizing Data using t-SNE". *Journal of Machine Learning Research* 9:86, 2008, pp. 2579–2605. URL: http://jmlr.org/papers/v9/vandermaaten08a.html.

30. Y. Netzer, T. Wang, A. Coates, A. Bissacco, B. Wu, and A. Y. Ng. "Reading Digits in Natural Images with Unsupervised Feature Learning". In: *NIPS Workshop on Deep Learning and Unsupervised Feature Learning 2011*. 2011. URL: http://ufldl.stanford.edu/housenumbers/nips2011_housenumbers.pdf.

31. S. J. Pan and Q. Yang. "A Survey on Transfer Learning". *IEEE Transactions on Knowledge and Data Engineering* 22:10, 2010, pp. 1345–1359. ISSN: 1558-2191. DOI: 10.1109/TKDE.2009.191. URL: https://ieeexplore.ieee.org/document/5288526 (visited on 08/17/2025).

32. A. Radford, J. W. Kim, C. Hallacy, A. Ramesh, G. Goh, S. Agarwal, G. Sastry, A. Askell, P. Mishkin, J. Clark, et al. "Learning transferable visual models from natural language supervision". In: *International conference on machine learning*. PmLR, 2021, pp. 8748–8763.

33. O. Russakovsky, J. Deng, H. Su, J. Krause, S. Satheesh, S. Ma, Z. Huang, A. Karpathy, A. Khosla, M. Bernstein, A. C. Berg, and L. Fei-Fei. *ImageNet Large Scale Visual Recognition Challenge*. 30, 2015. DOI: 10.48550/arXiv.1409.0575. arXiv: 1409.0575[cs]. URL: http://arxiv.org/abs/1409.0575 (visited on 03/19/2025).

34. R. Snow, B. O'Connor, D. Jurafsky, and A. Ng. "Cheap and Fast – But is it Good? Evaluating Non-Expert Annotations for Natural Language Tasks". In: *Proceedings of the 2008 Conference on Empirical Methods in Natural Language Processing*. Ed. by M. Lapata and H. T. Ng. Association for Computational Linguistics, Honolulu, Hawaii, 2008, pp. 254–263. URL: https://aclanthology.org/D08-1027/.

35. I. Sutskever, J. Martens, G. Dahl, and G. Hinton. "On the importance of initialization and momentum in deep learning". In: *Proceedings of the 30th International Conference on International Conference on Machine Learning - Volume 28*. ICML'13. event-place: Atlanta, GA, USA. JMLR.org, 2013, pp. III–1139–III–1147.

36. T. T. Tanimoto. *An Elementary Mathematical Theory of Classification and Prediction*. Google-Books-ID: yp34HAAACAAJ. International Business Machines Corporation, 1958. 10 pp.

37. J. Uijlings, T. Mensink, and V. Ferrari. *The Missing Link: Finding label relations across datasets*. 9, 2022. DOI: 10.48550/arXiv.2206.04453. arXiv: 2206.04453[cs]. URL: http://arxiv.org/abs/2206.04453 (visited on 04/23/2025).

38. A. Vaswani, N. Shazeer, N. Parmar, J. Uszkoreit, L. Jones, A. N. Gomez, L. Kaiser, and I. Polosukhin. *Attention Is All You Need*. 2, 2023. DOI: 10.48550/arXiv.1706.03762. arXiv: 1706.03762[cs]. URL: http://arxiv.org/abs/1706.03762 (visited on 08/17/2025).

39. M. Wang and W. Deng. "Deep visual domain adaptation: A survey". *Neurocomputing* 312, 2018, pp. 135–153. ISSN: 0925-2312. DOI: 10.1016/j.neucom.2018.05.083. URL: http://dx.doi.org/10.1016/j.neucom.2018.05.083.

40. *WordNet*. URL: https://wordnet.princeton.edu/homepage (visited on 08/06/2025).

41. H. Yang, A. Willis, D. Morse, and A. de Roeck. "Literature-driven Curation for Taxonomic Name Databases". In: *Proceedings of the Joint Workshop on NLP&LOD and SWAIE: Semantic Web, Linked Open Data and Information Extraction*. SWAIE 2013. Ed. by D. Maynard, M. van Erp, B. Davis, P. Osenova, K. Simov, G. Georgiev, and P. Nakov. INCOMA Ltd. Shoumen, BULGARIA, Hissar, Bulgaria, 2013, pp. 25–32. URL: https://aclanthology.org/W13-5207/ (visited on 08/17/2025).

42. A. R. Zamir, A. Sax, W. B. Shen, L. J. Guibas, J. Malik, and S. Savarese. "Taskonomy: Disentangling Task Transfer Learning". In: *IEEE Conference on Computer Vision and Pattern Recognition (CVPR)*. IEEE, 2018.

43. Y. Zhang and Q. Yang. "An overview of multi-task learning". *National Science Review* 5:1, 1, 2018, pp. 30–43. ISSN: 2095-5138. DOI: 10.1093/nsr/nwx105. URL: https://doi.org/10.1093/nsr/nwx105 (visited on 08/17/2025).

44. F. Zhuang, Z. Qi, K. Duan, D. Xi, Y. Zhu, H. Zhu, H. Xiong, and Q. He. *A Comprehensive Survey on Transfer Learning*. 23, 2020. DOI: 10.48550/arXiv.1911.02685. arXiv: 1911.02685[cs]. URL: http://arxiv.org/abs/1911.02685 (visited on 08/17/2025).

Eigenständigkeitserklärung

Hiermit erkläre ich, dass ich die vorliegende Masterarbeit selbstständig verfasst und gelieferte Datensätze, Zeichnungen, Skizzen und graphische Darstellungen selbstständig erstellt habe. Ich habe keine anderen Quellen als die angegebenen benutzt und habe die Stellen der Arbeit, die anderen Werken entnommen sind - einschließlich verwendeter Tabellen und Abbildungen - in jedem Fall unter Angabe der Quelle als Entlehnung kenntlich gemacht.

Bielefeld, den 6.9.2025

Buschkamper
(Unterschrift)